USDA

United States Department of Agriculture

Development of a Smart Timber Bridge (Phase III)

Moisture and Strain Sensor Investigation for Historic Covered Bridges

Brent M. Phares
Trevor L. Pence
James P. Wacker
Travis K. Hosteng

Forest Service
Forest Products Laboratory
General Technical Report
FPL–GTR–268
July 2019

In cooperation with the
United States Department of Transportation
Federal Highway Administration

A FHWA-NHCBP (National Historic Covered Bridge Preservation) publication

Abstract

Nationwide, bridges are deteriorating at a rate faster than they can be rehabilitated and maintained. This has resulted in a search for new methods to rehabilitate, repair, manage, and construct bridges. As a result, structural health monitoring and smart structure concepts have emerged to help improve bridge management. In the case of timber bridges, however, a limited amount of research as been conducted on long-term structural health monitoring solutions, and this is especially true in regards to historic covered timber bridges. To date, evaluation efforts of timber bridges have focused primarily on visual inspection data to determine the structural integrity of timber structures. To fill this research need and help improve timber bridge inspection and management strategies, a 5-year research plan to develop a smart timber bridge structure was undertaken. The overall goal of the 5-year plan was to develop a turnkey system to analyze, monitor, and report on the performance and condition of timber bridges. This report outlines one phase of the 5-year research plan and focuses on developing and attaching moisture sensors onto timber bridge components. The goal was to investigate the potential for sensor technologies to reliably monitor the in situ moisture content of the timber members in historic covered bridges, especially those recently rehabilitated with glulam materials. The timber-specific moisture sensors detailed in this report and the data collected from them will assist in advancing the smart timber bridge.

Keywords: Moisture content, sensor, timber, glulam, strain, reliability, accuracy

July 2019

Phares, Brent M.; Pence, Trevor L.; Wacker, James P.; Hosteng, Travis K. 2019. Development of a smart timber bridge (phase III): Moisture and strain sensor investigation for historic covered bridges. General Technical Report FPL-GTR-268. Madison, WI: U.S. Department of Agriculture, Forest Service, Forest Products Laboratory. 29 p.

A limited number of free copies of this publication are available to the public from the Forest Products Laboratory, One Gifford Pinchot Drive, Madison, WI 53726-2398. This publication is also available online at www.fpl.fs.fed.us. Laboratory publications are sent to hundreds of libraries in the United States and elsewhere.

The Forest Products Laboratory is maintained in cooperation with the University of Wisconsin.

English unit	Conversion factor	SI unit
foot (ft)	0.3048	meter (m)
inch (in.)	25.4	millimeter (mm)
kip (1,000 lbf)	4,448.2	newton (N)
kip per square inch (kip in^{-2})	6.89	megapascal (MPa)
pound, force (lbf)	4.4482	newton (N)
pound, mass (lb)	0.45359	kilogram (kg)
pound per square inch (lb in^{-2})	6.89	kilopascal (kPa)
$T_{°F}$	$T_{°C} = (T_{°F} - 32)/1.8$	$T_{°C}$

Contents

This study is part of the Research, Technology, and Education portion of the National Historic Covered Bridge Preservation (NHCBP) Program administered by the Federal Highway Administration. The NHCBP Program includes preservation, rehabilitation, and restoration of covered bridges that are listed or are eligible for listing on the National Register of Historic Places; research for better means of restoring and protecting these bridges; development of educational aids; and technology transfer to disseminate information on covered bridges in order to preserve the nation's cultural heritage.

This study is conducted under a joint agreement between the Federal Highway Administration–Turner-Fairbank Highway Research Center and the Forest Service–Forest Products Laboratory.

Federal Highway Administration Program Manager—Sheila Rimal Duwadi, P.E.

Forest Products Laboratory Program Manager—Michael A. Ritter, P.E.

Development of a Smart Timber Bridge (Phase III)

Moisture and Strain Sensor Investigation for Historic Covered Bridges

Brent M. Phares, Bridge Engineering Center Director
Trevor L. Pence, Graduate Student
Bridge Engineering Center, InTrans, Iowa State University, Ames, Iowa, USA

James P. Wacker, Research Engineer
USDA Forest Service, Forest Products Laboratory, Madison, Wisconsin, USA

Travis K. Hosteng, Wood Center Director
Bridge Engineering Center, InTrans, Iowa State University, Ames, Iowa, USA

1 Introduction

1.1 Background

Nationwide, bridges are deteriorating at a rate faster than they can be rehabilitated and maintained. This has resulted in a search for new methods to rehabilitate, repair, manage, and construct bridges. As a result, structural health monitoring and smart structure concepts have emerged to help improve bridge management. The idea is to develop and deploy systems that have sensors integrated into them to allow the condition and performance of the system to be reported on continuously and, generally, remotely. In the case of timber bridges, traditional condition assessments have been conducted by visual inspection and basic testing of the structure's members with maintenance decisions being based on the gathered information. To improve this situation, a conceptual smart timber bridge was developed with the purpose of improving the long-term performance, maintenance, and management of timber bridges.

Assessment of the smart timber bridge structural condition will be accomplished via measurement of flexural strains and evaluation of decay and deterioration by monitoring the moisture content (MC) of the structural members.

Several recent technological advances have resulted in the development of cost-effective sensing and communications systems, and the potential now exists to equip timber bridges with systems that report on their performance and condition using quantitative sensed information.

1.2 Objective and Scope

The objective of this report was to continue advancing timber-specific sensing capabilities and specifically to investigate the potential for sensor technologies to reliably monitor in situ wood MC in historic covered bridges, especially those recently rehabilitated with glulam materials. Furthermore, these findings will also benefit the development and refinement of other smart timber bridge technologies such as strain sensing technologies. The scope of the project included identifying potential sensing hardware for MC and evaluating its performance in the laboratory. In addition, strain sensors will be evaluated on full-scale laboratory beams, mounted both between the laminated layers as well as superficially on the beam surface, for long-term performance and accuracy.

1.3 Literature Review

This section presents a synopsis of previous research concerning the use of moisture sensors in civil engineering structures. Traditional methods of detecting moisture in wood will be discussed along with advanced methods currently in use. Although timber structures are the main focus of this research, an overview of concrete moisture sensors will be provided for completeness.

1.3.1 Traditional Methods for Determining Moisture Content in Timber Structures

The MC of wood, expressed as a percentage, is calculated by dividing the mass of water in wood by the mass of the ovendry wood (Forest Products Laboratory 2010). The purpose of measuring moisture is to determine areas with potential decay activity and to detect damage to untreated elements, such as roof and wall systems in covered bridge applications.

As wood decays, the electrical properties of the material are altered. Electrical-resistance-type moisture meters are the most common and simplest tool to measure the MC in wood. Moisture meters measure the electrical resistance at precise depths between two insulated probe pins embedded into the bridge member and relate the resistance to MC as shown in Figure 1.1. The variation shown by the shaded region in Figure 1.1 is generally caused by differences

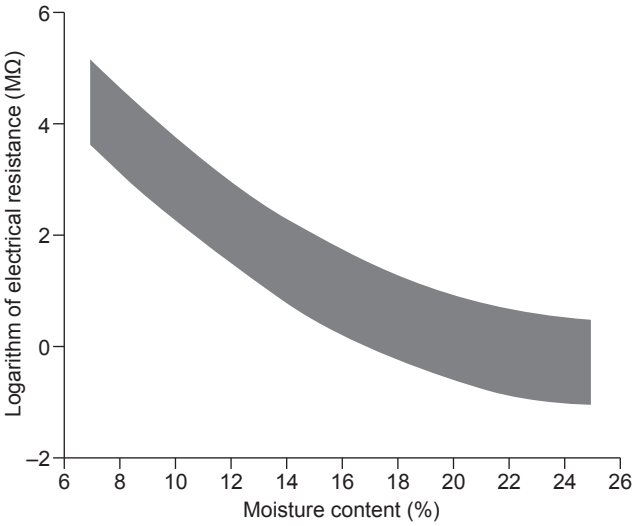

Figure 1.1. Relationship between electrical resistance and moisture content in wood (Forest Products Laboratory 1999, p. 3-22).

between wood species. For a given resistance, MC can vary as much as 10% if the species is unknown. Many commercially available moisture meters apply species and temperature correction factors to achieve more accurate MC readings. ASTM D4444-08 (ASTM 2008) outlines the procedure for using moisture meters to determine the MC in wood. Moisture meters have been proven to be an effective tool for timber bridge inspections. Although great for inspection purposes, moisture meters cannot be used to monitor the MC remotely and continuously over time, which is one of the goals of structural health monitoring.

Other ASTM standards are available to measure MC in wood. ASTM D4441 outlines four test methods to measure MC (ASTM 2007). Method A is intended as the sole primary method and is used when high levels of accuracy are needed (for example, research). Method A, the oven-dry method, requires pulverizing the wood material to saw dust. Then, the original mass of the sawdust is determined and compared with the oven-dry mass to determine the MC. Method B is also an oven-dry method; however, the method differs from method A in that the specimen can be a solid piece of wood instead of sawdust. Method C, the distillation method, is intended for materials that have been chemically treated for which oven-drying procedures induce greater error. This method uses an extraction apparatus and chemicals to measure the amount of water extracted from the specimen. The final method, Method D, accepts other methods to determine MC as long as the general practices and intent of the oven-dry and other methods are employed. Other methods include Karl Fischer titration, infrared (heating and absorption), microwave, nuclear magnetic resonance (NMR), and vacuum oven-drying. These methods are for laboratory experiments and therefore are not feasible for the in situ measurements required for this work.

1.3.2 Monitoring the Moisture Content of Timber Bridges

Treteknisk (Norwegian Institute for Wood Technology, Oslo, Norway) previously instrumented five Norwegian timber bridges to monitor the MC over time. They instrumented the bridges by embedding relative humidity–temperature sensors into various timber members. The MC of timber depends on both the relative humidity and temperature of the air surrounding it. Therefore, by embedding a relative humidity–temperature sensor in a small void within the wood, equilibrium moisture content (EMC) can be obtained assuming the MC of the wood is in equilibrium with the humidity of the air. The relationship between relative humidity, temperature, and EMC is shown in the following equation (Dyken and Kepp 2010):

$$\mathrm{EMC} = \frac{(1{,}800Kh)}{W(1-Kh)} + \frac{K_1Kh + 2K_1K_2K^2h^2}{1 + K_1Kh + K_1K_2K^2h^2} \qquad (1.1)$$

where

$W = 330 + 0.452T + 0.00415T^2$,

$K = 6{,}034 + 0.000463T - 0.000000844T^2$,

$K_1 = 6.34 + 0.000775T - 0.0000935T^2$,

$K_2 = 1.91 + 0.0407T - 0.000293T^2$,

T is temperature (°F), and

h is relative humidity.

Results from testing yielded MC that varied significantly with temperature. Furthermore, EMC values varied substantially within a short period of time, which was considered improbable. However, the long-term averages of MC appeared to be reasonable. A conclusion was made that the influence of temperature artificially skewed the MC that was calculated using Equation (1.1). In an effort to obtain more accurate results, laboratory tests were carried out to establish a new formula.

The idea of the laboratory tests was to keep the MC constant, vary the temperature, and see how the relative humidity changed. Various specimens with known MCs were embedded with humitters (Vaisala, Helsinki, Finland) and completely sealed off with adhesive tape to keep the MC constant. After four series of laboratory tests, a substantial amount of data were available. The specimens had MCs that ranged from 6.2% to 21.3% and the temperature ranged from 85 to 86.5 °F. The test results confirmed that Equation (1.1) could be used as an approximation to calculate MC; however, a new equation had to be developed to eliminate the short-term temperature effects on the calculated MC. To establish a new formula, MC was plotted as a function of relative humidity at various temperatures. A quadratic polynomial best fit line was chosen to approximate the data. The following is the new equation:

$$\mathrm{MC}(\mathrm{RH}, T) = \left((a_\mathrm{A}T^2 + b_\mathrm{A}T + c_\mathrm{A})\mathrm{RH}^2\right) + \left((a_\mathrm{B}T^2 + b_\mathrm{B}T + c_\mathrm{B})\right) + (a_\mathrm{C}T^2 + b_\mathrm{C}T + c_\mathrm{C}) \quad (1.2)$$

where

$a_\mathrm{A} = 0.57 \times 10^{-6}$,

$a_\mathrm{B} = 70.3 \times 10^{-6}$,

$a_\mathrm{C} = 2.0553 \times 10^{-3}$,

$b_\mathrm{A} = 29.34 \times 10^{-6}$,

$b_\mathrm{B} = 2.8933 \times 10^{-6}$,

$b_\mathrm{C} = 2.4551 \times 10^{-3}$

$c_\mathrm{A} = 1.17007 \times 10^{-3}$

$c_\mathrm{B} = 87.6041 \times 10^{-3}$,

$c_\mathrm{C} = 4.181162$,

T is temperature (°C), and

RH is relative humidity (%).

The new equation was applied to the five Norwegian bridges mentioned earlier. Equation (1.2) resulted in less MC variation over time compared with Equation (1.1). However, large temperature variations caused Equation (1.2) to fluctuate slightly. In addition, the new equation indicated that the wood MC was slightly higher than what Equation (1.1) implied. However, both equations were below the ambient EMC, which implies the structure dries out with time. A conclusion was drawn that wood may not attain an EMC relating to the ambient climate. Therefore, one should never assume the MC of wood based on ambient conditions.

1.3.3 Monitoring the Performance of Timber Bridges over the Long Term

The USDA Forest Service, Forest Products Laboratory (FPL), conducted a preliminary study to monitor the performance of timber bridges over the long term (Wacker and others 2007). One component of the study was to evaluate the performance of wood moisture sensors. The goal was to outline sensor types and features needed to obtain reliable data to successfully monitor moisture in timber bridges.

The approach was to subject a small-scale birch beam to controlled moisture conditions (70 °F and 12% relative humidity) and evaluate the change in the wood MC over a 60-day period. The specimen was a 5- by 5- by 48-in. birch beam equipped with two different types of moisture sensors. The first type was a Vaisala relative humidity–temperature sensor. Six of the relative humidity–temperature sensors were embedded along the beam at different depths. In addition to the relative humidity–temperature sensors, a remote wireless resistance pin sensor was installed on the surface of the beam and monitored during the same period. As a control reference, the beam was weighed continuously during the 60-day period to obtain a theoretical MC.

The results indicated that the MC recorded by the sensors varied with the depth of the sensor. In addition, the sensors were limited in the upper range to the fiber saturation point. The beam started with approximately 75% MC, and the fiber saturation point is approximately 25%; therefore, the sensors did not provide meaningful data until the MC was below 25%. The study provided preliminary work with regard to the development of wood moisture sensors, offering a starting point for future work.

1.3.4 Long-Term Monitoring of Timber Moisture Content below the Fiber Saturation Point using Wood Resistance Sensors

In many applications, commercial resistance-type moisture meters have their drawbacks, including calibration, polarization, and the constraint of measuring points. In Dai and Ahmet (2001), a moisture sensor was designed to meet the stringent requirements with respect to accuracy. The designed sensors, or probes, consist of two pairs of silver-painted brass screw-type electrodes inserted into a wood buffer 0.5 in. apart. These parallel electrodes, equivalent to a network of six resistances, provide the potential for measuring moisture gradients. The probes were tested in beech samples. The probes were inserted into 0.4-in.-diameter holes, and the holes were sealed to ensure the outside atmosphere did not affect the sensor environment. The results of the study showed that the moisture probes compared well with readings obtained from commercially available moisture meters. Furthermore, the prototype sensor was able to be wired into a data logging system, making the probes ideal for timber applications requiring accurate long-term moisture measurements. A moisture sensor of similar configuration was used during the work described herein.

1.3.5 Demonstration of a Fiber-Optic Sensing Technique for Measuring Moisture Absorption in Concrete

In Yeo and others (2005), a fiber-optic-based humidity sensor was developed and used for the measurement of moisture absorption in concrete. The humidity sensor used in this work was based on expansion principles, using a fiber Bragg grating (FBG). The humidity sensor was created by coating an optical fiber containing an FBG with a moisture-sensitive polymer that absorbs moisture, causing it to swell. This swelling stretches the fiber and causes a strain in the FBG. This process changes the wavelength of the reflected signal, which can be monitored using an optical spectrum analyzer or any other similar wavelength-based interrogation technique.

To fabricate the sensors used in this work, the fiber optic first had a fiber Bragg grating (FBG) written in B/Ge co-doped photosensitive fibers using the phase mask technique. The FBG samples were then annealed at 392 °F for 7 h and treated with a silane coupling agent prior to the coating. A multiple-dip coating process involving 20 layers was used to coat the FBG with polyimide.

Protection of the sensor was a concern because of the fragile nature of the fiber and the need to use it as a probe. Protection was achieved by using a thin metal tube to cover the sensor and having holes drilled along each side to allow the free circulation of fluids. The metal tube was fixed to the sensor using epoxy resin.

To test the sensors, standardized cylindrical samples of concrete were made with a diameter and length of 3.9 in. The cylinders were cast with a 0.16-in.-diameter hole at the center to a depth of 3.2 in., creating a void for the sensor to rest in. For each test, a sample was set up with the probe placed in the center of the concrete cylinder. The entry point of the probe was then filled with malleable wax, to prevent any water from seeping in and to keep room humidity from having any effect on the measurements. The sample was left for approximately 1 h to allow the sensor to reach equilibrium. Next, the sample was placed in a water bath with a controlled water level and the temperature was regulated at 73.4 °F. The characteristic wavelength of the FBG was then determined. The relative humidity was then calculated using a previously obtained calibration chart.

The laboratory results showed that the fiber-optic-based humidity sensors can be used effectively to monitor moisture changes in different concrete samples. This indicates that there is a potential new application of the sensor system, which could contribute to the integrity of civil engineering structures in general.

2 Small-Scale Sensor Evaluation

This chapter presents the evaluation of three moisture sensors suitable for continuously measuring MC in timber structures. Information on each moisture sensor and techniques for embedding and attaching the sensors are discussed. In addition, the testing procedure followed to evaluate sensor performance is provided along with results and recommendations.

2.1 Moisture Sensors

Three commercially available moisture sensors were evaluated for survivability and accuracy of measurements. The first sensor was an SHT71 relative humidity–temperature sensor (Fig. 2.1) from Sensirion (Staefa, Switzerland). A unique capacitive sensor element is used for measuring the relative humidity, whereas temperature is measured by a band-gap sensor. Each sensor is calibrated in a precision humidity chamber, and calibration coefficients are programmed into a one-time programmable (OTP) memory on the chip. These coefficients are used to internally calibrate the signals from the sensors. As mentioned previously, EMC can be determined by measuring the temperature and relative humidity within a small void in the wood. The following equation was used to calculate the MC:

$$\mathrm{MC} = \left(\frac{R}{5\times10^{9}}\right)^{\frac{1}{-7.145}} \qquad (2.1)$$

where

MC is moisture content at 73.4 °F (%) and

R is resistance (MΩ).

The second sensor chosen for evaluation was a point moisture measurement (PMM) sensor from Structure Monitoring Technology (SMT Research Ltd., Vancouver, British Columbia, Canada) (Fig. 2.2). The PMM sensor measures the electrical resistance between two #6 screws driven into the wood. The electrical resistance is then converted to MC based on an empirical relationship established by previous research, shown by Equation (2.1). The MC is then corrected for species and temperature based on the following equation (Pfaff and Garrahan 1984) (The a and b species correction coefficients may be found in published tables by the manufacturer, and an integrated temperature sensor allows for a temperature correction):

$$\mathrm{MC}_{\mathrm{corrected}} = \left(\left(\frac{\mathrm{MC} + \left(0.567 - 0.0260x + 0.000051x^{2}\right)}{0.881(1.0056^{x})}\right) - b\right) \div a \qquad (2.2)$$

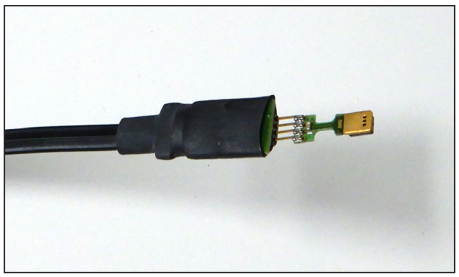

Figure 2.1. Relative humidity–temperature sensor.

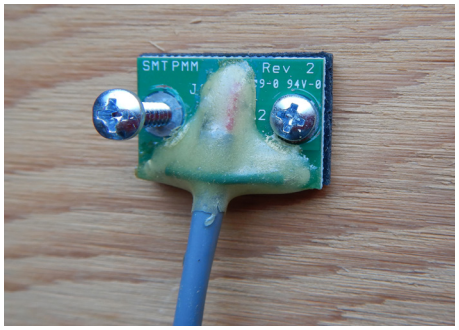

Figure 2.2. Point moisture measurement sensor.

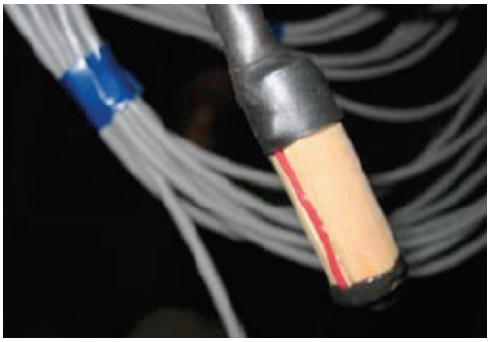

Figure 2.3. Embedded moisture sensor (copyright, Structure Monitoring Technology, SMT Research Ltd., Vancouver, British Columbia, Canada). Used with permission.

where

MC is moisture content at 73.4 °F (%),

x is temperature of the wood (°C), and

a,b are species correction coefficients.

The final sensor chosen for evaluation was an embedded moisture sensor (EMS) (Fig. 2.3) and was also from Structure Monitoring Technology. The EMS is used to perform an indirect measurement of moisture levels in materials not compatible with standard measurement techniques. The sensor is essentially a wooden plug with electrodes attached to each end. The electrical resistance of the plug is measured to determine the relative MC of the surrounding area through capillary absorption. The MC of the EMS was also calculated using Equations (2.1) and (2.2).

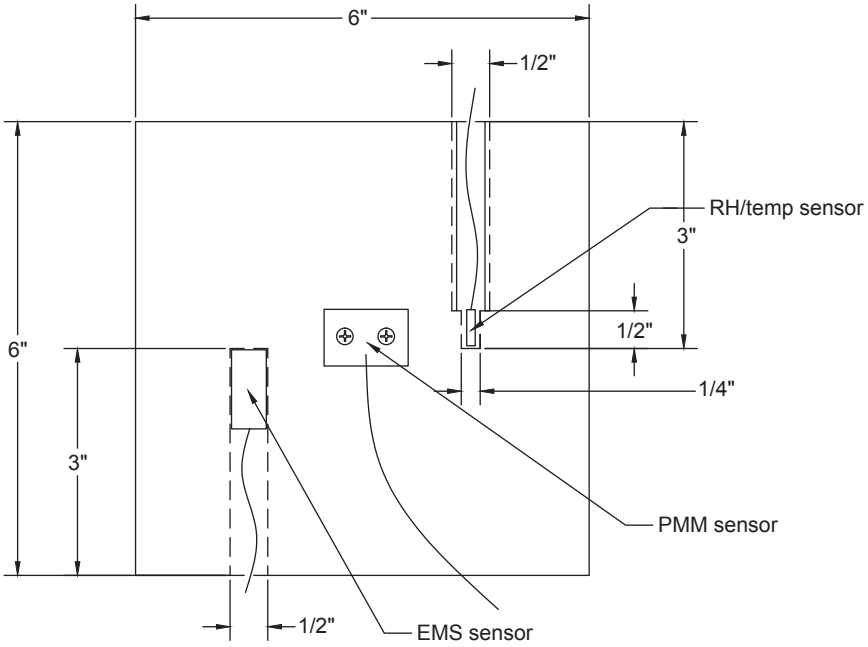

Figure 2.4. Typical test specimen (PMM, point moisture measurement; EMS, embedded moisture sensor).

2.2 Testing Program

The following section is a description of the testing program followed to evaluate the survivability and accuracy of the selected moisture sensors. During testing, four 6- by 6- by 2-in. southern yellow pine specimens were tested under varying relative humidity and temperature conditions. All specimens had each of the three previously described moisture sensors installed.

2.2.1 Installation

To embed the relative humidity–temperature sensors, a 1/2-in.-diameter hole was drilled 2-1/2 in. deep. Next, a 1/4-in.-diameter hole was drilled an additional 1/2 in. deep to create a void for the sensor to rest in. A 3/8-in. plastic sleeve was inserted to the 2-1/2-in. depth to restrict moisture penetration into the sensor void from other areas of the specimen. The sensor was then inserted into the hole, resting in the void. Silicon sealant was placed over the top of the sleeve to restrict the intrusion of ambient conditions into the sensor void.

A similar technique was used to install the EMS. A 9/16-in.-diameter hole was drilled 3 in. deep, and the sensor was inserted to the full depth. The sawdust from the drill hole was used to fill the space from the sensor to the surface. The top of the hole was then sealed with silicone sealant.

The PMM sensors were installed by simply driving two #6 3/4-in. screws through the sensor and into the wood. The sensors were oriented such that the screws were lined parallel to the grain direction. Figures 2.4 and 2.5 illustrate the sensor locations on the wood specimens.

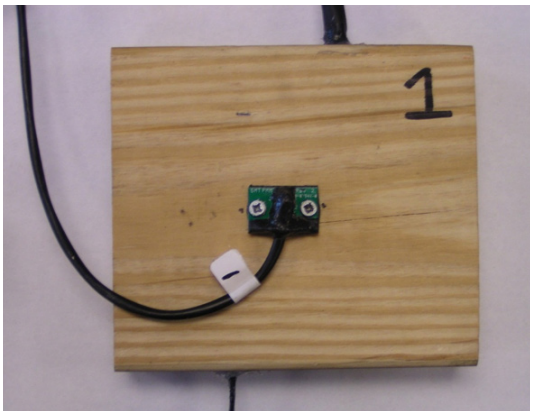

Figure 2.5. Specimen 1 (typical of all specimens).

2.2.2 Wiring

To integrate the sensors into a bridge monitoring system, the sensors must be wired into a data logger that is capable of reading other sensor types (for example, strain, accelerometers, thermistor, etc.). The PMM and EMS sensors were wired to an off-the-shelf data logger capable of reading other sensor types. However, the relative humidity–temperature sensor was unable to be wired to the logger because of the proprietary digital output signal. Thus, the data logger specific to the relative humidity–temperature sensor was used instead to collect data. Each logger took a reading every 30 min.

Most logging systems are not able to read the high resistances (hundreds of Mohms) required to determine the MC of wood. Therefore, a unique wiring system had to be

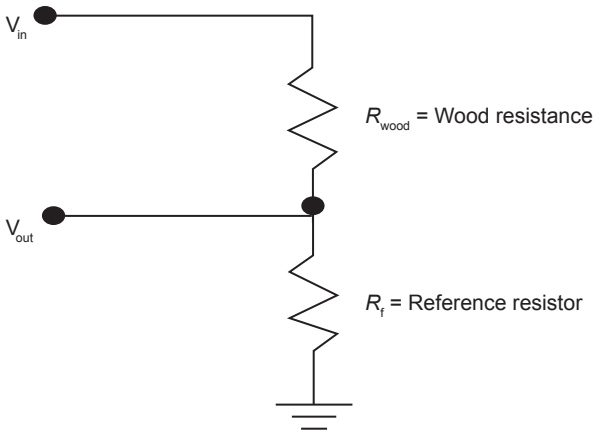

Figure 2.6. Wiring schematic.

Figure 2.7. Specimens in the 20% equilibrium moisture content room.

developed to record the high resistance values. The wiring schematic is illustrated in Figure 2.6. By using a reference resistor (R_f), the voltage drop across the sensor can be measured. Using Ohm's law and algebraic manipulation, the following equations were developed to determine wood resistance (R_{wood}):

$$X = \frac{V_{out}}{V_{in}} \quad (2.3)$$

$$R_{wood} = \frac{R_f(1-X)}{X} \quad (2.4)$$

2.2.3 Testing Conditions

The specimens were subjected to varying moisture conditions to evaluate the survivability and response of the sensors. All moisture testing was done at FPL in Madison, Wisconsin, USA. First, the four specimens were placed in an environmentally controlled room with a temperature of 80 °F and 90% relative humidity. These conditions correspond, theoretically, to an EMC of 20%. Figure 2.7 shows the four specimens in the 20% EMC room. After the EMC was reached, the specimens were placed in a drying room at 80 °F and 37% relative humidity until the corresponding EMC of 7% was reached. Lastly, the specimens were placed back in the 20% EMC room. As a reference, the MC was periodically checked with a commercially available moisture meter. Additionally, the specimens were periodically weighed to obtain gravimetric MCs; however, the wires attached to the sensors are believed to have absorbed moisture, resulting in inaccurate readings, although this was not experimentally confirmed.

2.3 Results

Figures 2.8 to 2.11 summarize the sensor measurements with time for each specimen. Again, the specimens were all the same size and the moisture sensors were placed in approximately the same location in all specimens.

The circles in the figures represent MC obtained by a conventional moisture meter (Delmhorst Instrument Co., Towaco, New Jersey, USA).

From the figures, the point at which the specimens changed environmental rooms is easily observed by a sudden drop or increase in MC (increase starting at 1/5/12; decrease starting at 3/25/12; increase starting at 5/4/12). Another obvious trend in the figures is the MC of each sensor relative to the others. The relative humidity–temperature sensors were consistently higher than the other two sensors, the PMM sensors fell in the middle, and the EMS were consistently lower than the other two sensors. As noted in the figures, some data did not compare well with the moisture meter. Discussions of each sensor performance and errors that may have contributed to the differences are subsequently described. The cause(s) of the sharp decreases in MC around 5/20/12 and 6/11/12 are unknown.

2.3.1 Relative Humidity–Temperature Sensor Performance

The relative humidity–temperature sensors appeared to be the most accurate compared with the moisture meter. The sensor was able to read MCs near 20%. The threshold MC for incipient decay in wood is around 20%; therefore, accuracy around 20% MC is important. Another advantage of the sensor is that it experiences less noise compared with the other sensors. Figures 2.8 to 2.11 show a smooth line with little variation between successive points. Although this sensor has many advantages, one disadvantage is its inability to be wired into an off-the-shelf data logging system equipped with other sensor types.

2.3.2 Point Moisture Measurement Sensor Performance

The PMM sensor appeared to be most accurate at lower MC readings. The sensor was unable to read an MC of 20%, falling short by approximately 5%. The main difference between the readings from the PMM sensor and the moisture meter was insertion depth of the pins.

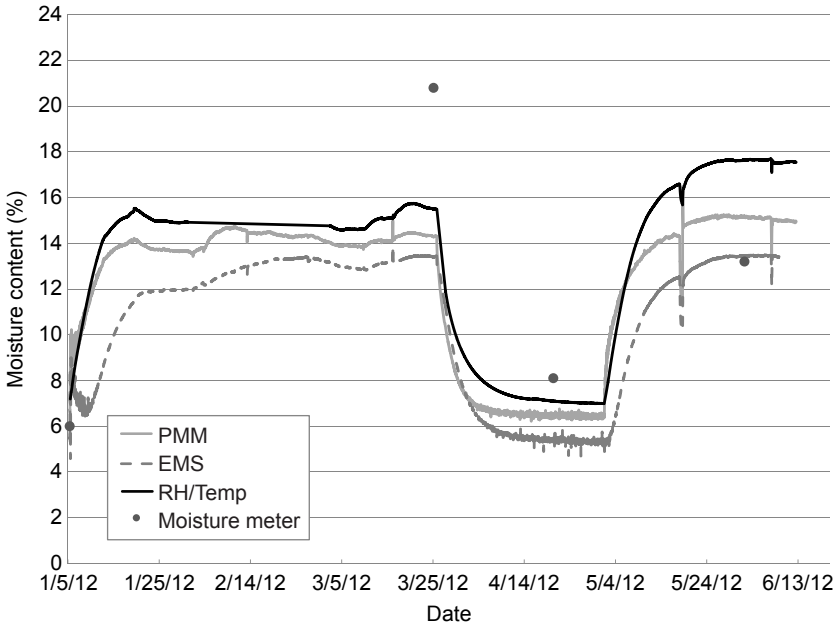

Figure 2.8. Specimen 1 moisture content with time (PMM, point moisture measurement; EMS, embedded moisture sensor; RH, relative humidity).

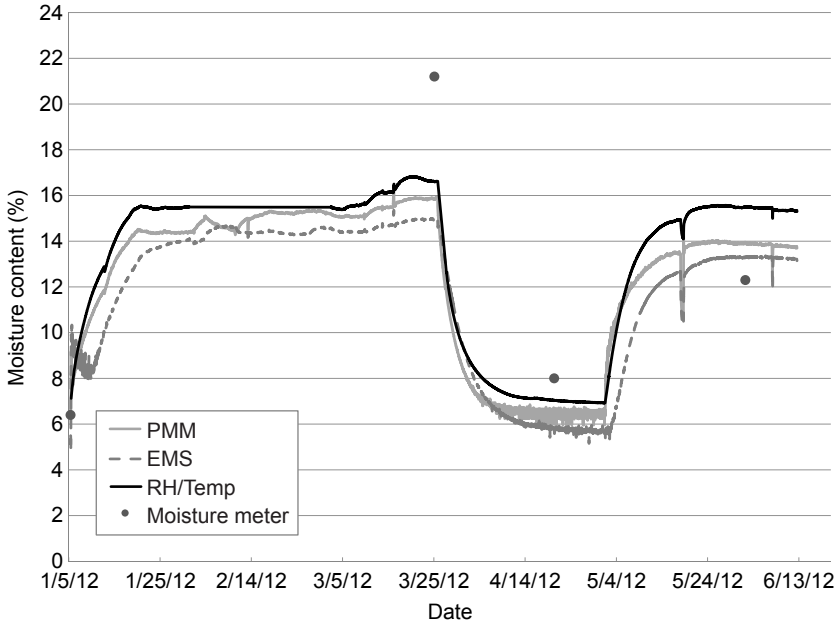

Figure 2.9. Specimen 2 moisture content with time (PMM, point moisture measurement; EMS, embedded moisture sensor; RH, relative humidity).

The moisture meter is equipped with insulated pins that measure the electrical resistance only at the tip of the pins. In other words, the MC is obtained at the exact location of the penetration depth. Conversely, the PMM sensors are equipped with noninsulated screws that measure the electrical resistance throughout the whole length of the screw. The manufacturer of the PMM sensor recommends using a nylon tube that goes around the screw just prior to the desired depth of penetration. Although ensuring the appropriate penetration depth orientation relative to grain would probably not make up for the 5% MC difference, it does provide a partial explanation for the differences between the moisture meter and PMM readings. Furthermore, according to the manufacturer, readings taken only inches away from each other could differ by 3% to 5% MC. One advantage of the PMM sensor compared with the other sensors is ease of installation. Predrilled holes and sealing the sensor are not required, saving time and difficulties in field installation.

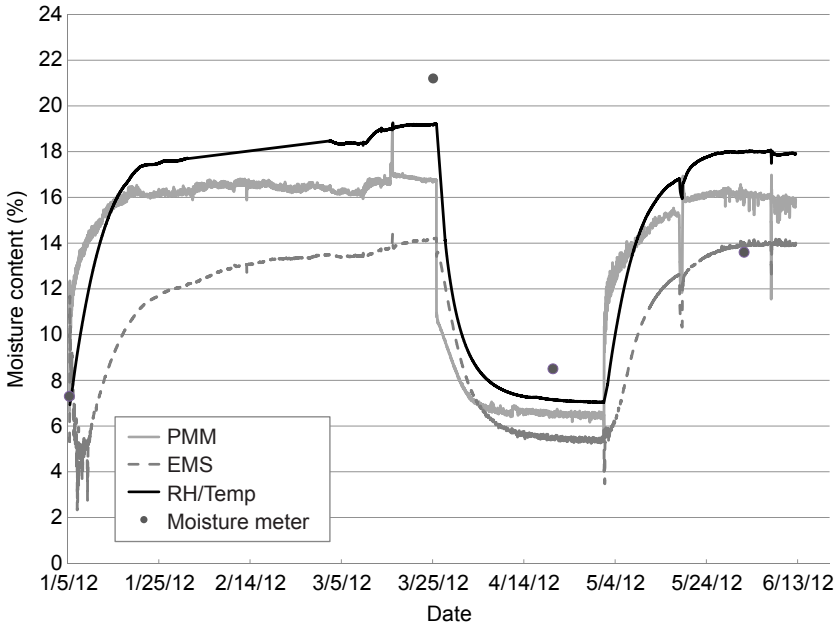

Figure 2.10. Specimen 3 moisture content with time (PMM, point moisture measurement; EMS, embedded moisture sensor; RH, relative humidity).

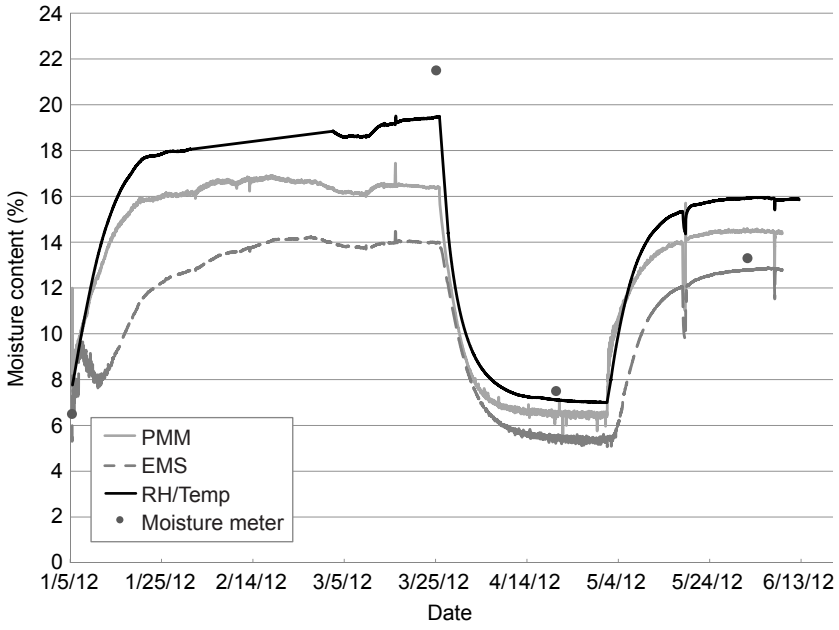

Figure 2.11. Specimen 4 moisture content with time (PMM, point moisture measurement; EMS, embedded moisture sensor; RH, relative humidity).

2.3.3 Embedded Moisture Sensor Performance

The EMS did not perform as well as the PMM and the relative humidity sensors. The EMS was unable to record readings at the 20% MC threshold, falling short by as much as 8%. Discussions with the EMS manufacturer revealed that the EMS is usually used in concrete and sandstone materials in which moisture level is a concern but accurate MC measurements of the material are not. Although the EMS can be used in wood materials, the manufacturer recommends the PMM sensor rather than the EMS to obtain more accurate MC measurements.

2.3.4 General Remarks

Based on the previous discussion, a recommendation was made to proceed with evaluation of the PMM sensor. Although the relative humidity–temperature sensor gave more accurate results, the PMM sensor was able to be wired into a data logging system capable of reading other sensor types. Furthermore, future calibration of the PMM sensor could be conducted to achieve better accuracy. Survivability of the PMM sensor under repeated loading is discussed in the next chapter.

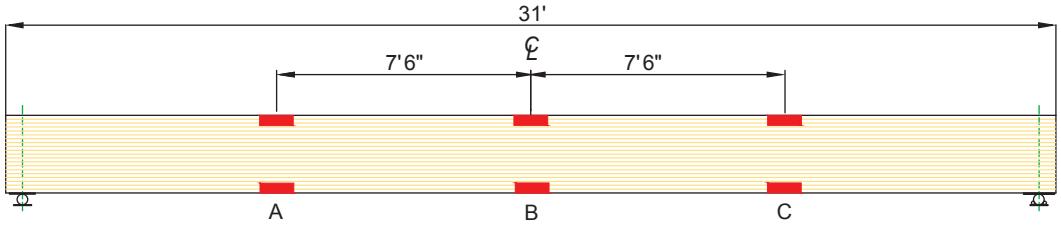

Figure 3.1. Strain gage locations along the length of the girder.

3 Full-Scale Glulam Specimens

In the previous chapter, the PMM sensor was selected for further evaluation based on the sensors performance under varying environmental conditions and the sensors ability to be integrated into a broader monitoring system. In this chapter, the PMM sensor and foil strain gage packages are evaluated for survivability under repeated loading. Two full-scale glued-laminated (glulam) timber girders were assembled with foil strain gages and PMM sensors. The girders were fatigue tested to one million cycles with two-point loading simulating typical truck service stress levels. The operability of both sensor types (strain and moisture) under repeated loading was then evaluated.

3.1 Installation of Strain Sensors During the Glulam Girder Manufacturing Process

An earlier phase of this project developed a technique to attach and embed fiber-optic strain gages within a glulam girder (Phares and others 2010). For simplicity and repeatability of results, the girders used in this report are identical in dimensions to the girders tested in the earlier phase with different gage types and installation techniques used as subsequently detailed. The selected girders had a rectangular cross section of 27-1/2 by 6-3/4 in. and a length of 31 ft. The girder was fabricated with a beam layup of 24F-V8 by a local glulam manufacturer. The girders consisted of 20 laminates symmetrically balanced in lumber quality and strength through the depth. The first girder, Girder 1, was constructed using Southern Pine laminates and was left untreated. The second girder, Girder 2, consisted of Douglas-fir laminates and was pressure treated using pentachlorophenol. The purpose of treating the second girder was to observe if exterior gages adhere to treated timber. The locations of the strain gages embedded in and attached to Girder 1 are shown in Figures 3.1 and 3.2.

3.2 Girder 1

3.2.1 Strain Gage Package Type

A mechanism for attaching strain gages to timber was recommended in previous research (Phares and others 2010). The recommended package consisted of a stainless steel shim as the backing material and a bare FBG strain sensor as the sensor type. However, the study found that

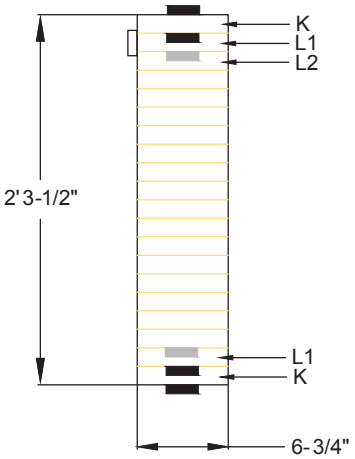

Figure 3.2. Sensor locations at cross sections A, B, and C. (In the top half of the beam, the sensors were placed on the top side of L1 and L2. In the bottom half, the sensors were placed on the top side of K and L1.)

the FBG sensors were easily damaged in the fabrication process because of the fragile nature of the sensors. Electrical-resistance-type strain gages, also called foil strain gages, were used in place of the FBG sensors to increase survivability of the gages through the glulam fabrication process. The stainless steel shim was rectangular in shape and had dimensions of 8-1/2 by 7/8 in. with a thickness of 0.005 in. The dimensions of the shim were developed to resist the shear stresses and to allow for the redistribution of localized strain irregularities between the sensor and the wood laminates.

3.2.2 Assembling the Shim Sensors

The procedure for assembling the shim sensors was as follows:

A 0.005-in.-thick stainless steel shim was cut to the dimension of 8-1/2 by 7/8 in., and alignment marks were drawn in the center where the gage was to be placed.

Fine-grade sandpaper was used to roughen the approximate location of the gage.

The roughened area was wiped with acetone to clean the surface.

The foil gage was removed from its transparent envelope by grasping the edge of the gage backing with tweezers, and it was placed bonding side down on a chemically clean glass plate.

With PCT-2M gage installation tape (Micro-Measurement, Vishay Precision Group, Malvern, Pennsylvania, USA), one end of the tape was tacked to the glass plate behind the gage and wiped forward onto the gage. The tape was carefully lifted at a shallow angle, bringing the gage up with the tape.

The tape–gage assembly was wiped onto the shim in the correct location (the center).

One end of the tape was lifted at a shallow angle until the gage was free from the shim surface.

Adhesive was applied to the back of the gage and/or shim surface, and the gage was slowly brought back down over the alignment marks on the shim.

Firm pressure was held for approximately 1 min.

The tape was removed by slowly pulling the tape back directly over itself.

If the gages were not prewired, the wire was soldered onto the terminals provided on the gage.

The gage was coated with polyurethane to add a protective layer.

Butyl rubber tape was used to cover the gage. This prevented moisture from penetrating the gage area.

Finally, the gage area was covered with foil.

To save time while fabricating the glulam girder, the shim sensors were preassembled prior to arriving at the glulam manufacturing facility.

3.2.3 Installing the Shim Sensors

The procedure for assembling a glulam girder with the embedded shim sensors is outlined below, as well as in Figures. 3.3 to 3.6.

The preliminary stages of the fabrication process remain the same:

On-site lumber was dried to approximately 16% MC.

Lumber was graded.

Sawn lumber was end-jointed with finger joints to achieve the given length. Glue needed to be cured to achieve adequate strength of the joint.

Each laminate was planed on both sides to ensure clean, parallel surfaces for gluing.

After planing, four internal laminates were prepared for sensor installation (Fig. 3.2). A typical laminate is illustrated in Figures 3.3 to 3.5. Three areas along the length of the each laminate were routed 1/4 in. deep, 1 in. wide, and 12 in. long to hold the shim sensor. A groove 1/4 in. wide and 1/4 in. deep was also routed to hold the wire. All wires were run in the same direction on all laminates. Furthermore, the wires met in the recessed area as shown in detail B on Figure 3.3.

After the laminates were routed in the appropriate locations, the shim sensor was glued in the recessed area as detailed in Figure 3.6.

Figure 3.7 illustrates the final steps in the fabrication process. After allowing the Loctite-426 adhesive (Henkel AG & Company, Düsseldorf, Germany) to cure for 24 h, the laminates were glued and placed carefully into the clamping apparatus. As usual, the clamps were applied at 100 lb/in^2 for approximately 24 h.

After the girder was removed from the clamping system, the sides were planed to remove beads of resin. Other finishing steps may have occurred to enhance the appearance of the girder. However, the ends of the girder where the wires exit remained untouched.

After the construction of Girder 1, a multimeter was used to verify that all sensors were operative. Furthermore, the gages were checked in the laboratory upon arrival of the girder. It was concluded that all 12 gages survived the construction, handling, and transportation process. After Girder 1 arrived in the lab, exterior mounted gages and moisture sensors were attached using the same methods as previously described. Three moisture sensors were installed at the cross sections A, B, and C as noted in Figure 3.1. However, the sensors were unable to be wired to the data acquisition system; therefore, the moisture sensors were inoperable during testing. The moisture sensors were operable during the Girder 2 fatigue test, which will be subsequently discussed.

3.2.4 Testing Program

Girder 1 was fatigue tested to evaluate operability of the sensors under repeated loadings. The girder was cycled at a rate of 0.5 Hz for approximately 1 million cycles with a peak load of 24,000 lb. The 31-ft girder was supported by one pin and one roller located 6 in. from each girder end. The girder was tested in bending by the two-point loading method as shown in Figure 3.8. To apply the load at two points, a steel load frame was positioned at midspan and a 10-ft structural tube (6- by 6- by 1/4-in. spacer beam) was used to transfer the load from the actuator to two points on the girder spaced 9 ft apart. Furthermore, two inverted T frames were fabricated and positioned to prevent instability during loading (Fig. 3.9).

Initially, data were collected for 5 min every hour at a rate of 10 Hz. However, the collection rate was decreased to 1 min every hour at 10 Hz to decrease the amount of data.

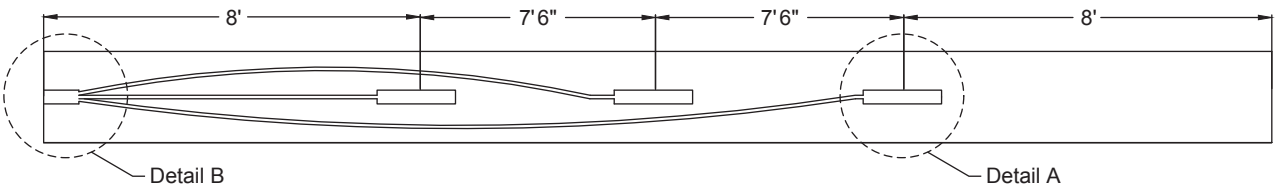

Figure 3.3. Recessed area on a typical laminate.

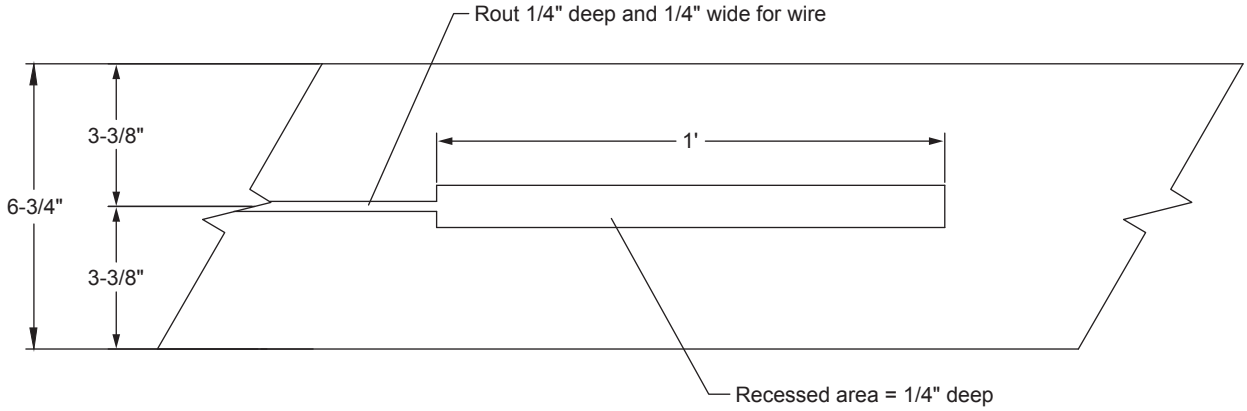

Figure 3.4. Detail A from Figure 3.3.

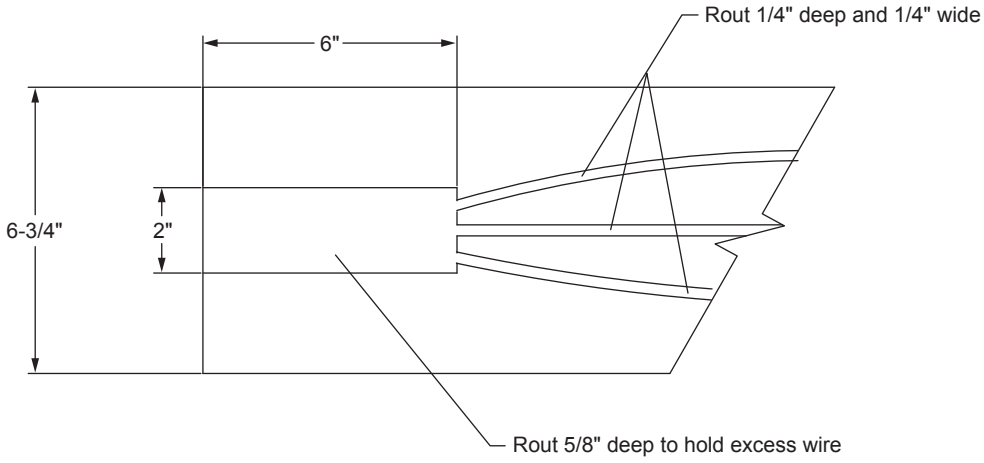

Figure 3.5. Detail B from Figure 3.3.

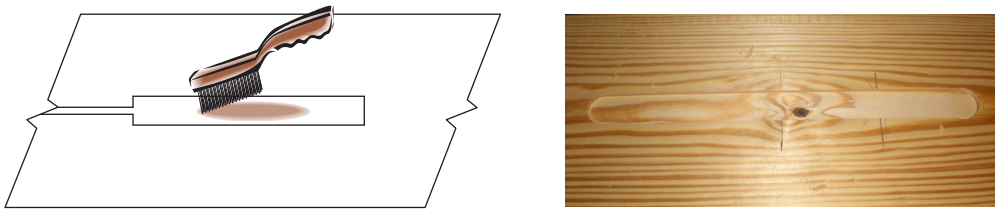

i. Clean laminate by brushing off any debris.

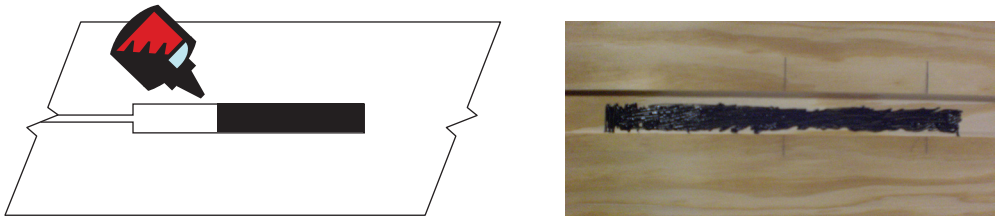

ii. Apply Loctite-426 adhesive evenly throughout the recessed area.

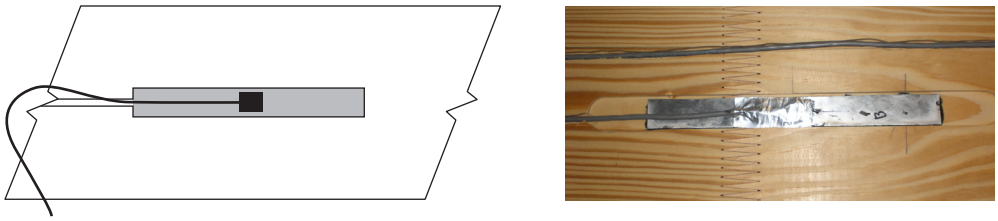

iii. Carefully insert the shim sensor with the foil gage facing up (shown in black).

iv. Apply moderate pressure to the shim sensor for 24 hours using a 1-inch-thick steel plate. Note: this step was skipped for Girder 1. Instead, pressure was incorrectly applied by hand for approximately 2 minutes.

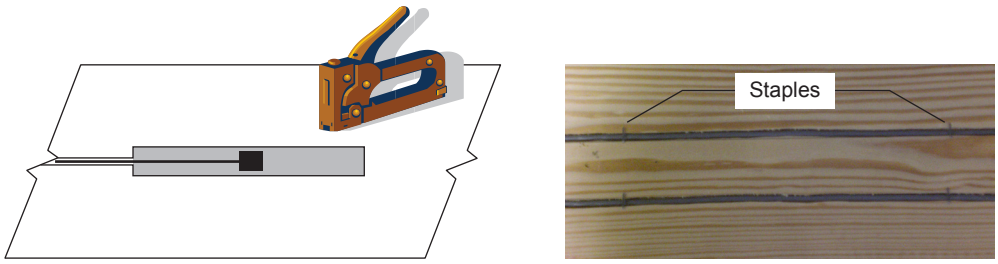

v. Insert the wire into the 1/4-inch groove and staple across the groove at 1-foot increments along the length of the laminate to hold the wire in place.

Figure 3.6. Gage installation procedure.

Figure 3.7. Clamping and planing the girder: (a) aligning the laminates in the clamping apparatus; (b) checking the gages with a volt meter; (c) planing the beam; (d) finished beam.

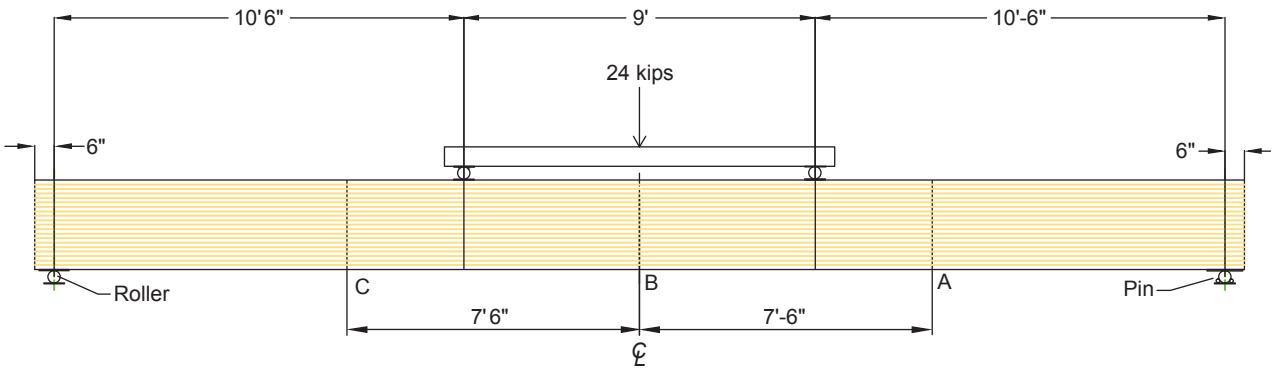

Figure 3.8. Test set-up.

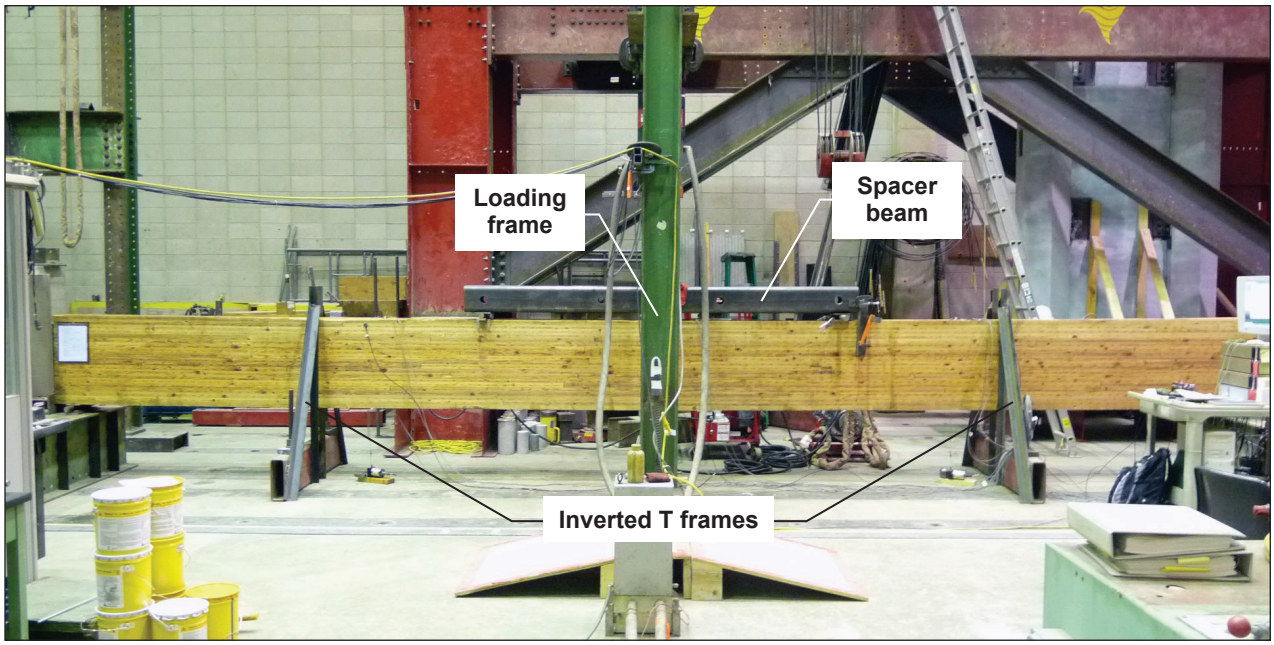

Figure 3.9. Test set-up.

3.2.5 Results

As the beam cycles, the predicted response of the gages is a constant peak strain; however, a slight increase in peak strain may occur as the beam fatigues and cracks develop, thereby decreasing overall beam stiffness. Throughout the test, nine of the eighteen gages did not maintain a steady peak strain and exhibited unusual behavior, thus indicating defective gages. The trends of the defective gages were not consistent among each other. For example, some gages had a sudden increase in peak strain whereas others gradually decreased in peak strain. Furthermore, some gages recorded unusually high strains whereas others were abnormally low. The erratic behavior of the gages is illustrated in Figures 3.10 and 3.11. In addition, seven of the nine defective gages began behaving erratically within the first 100,000 cycles of the test, indicating that something changed early on in the test. Table 3.1 lists the status of the gages and an approximate point of failure. The point of failure is defined as the number of cycles at which unusual behavior initiated.

The test was stopped at approximately 200,000 cycles to examine the exterior gages and strain history plots to troubleshoot the problem. As the girder was cycled, parts of the shim backing material were observed to have lifted from the timber surface, indicating insufficient adhesion. A conclusion was made that insufficient adhesion between the shim and timber surface led to the erratic behavior of several gages. An improved sensor preparation and installation procedure was needed to provide long-term adhesion between the shim and timber.

Most of the adhesive adhered to the wood and not the stainless steel shim (Fig. 3.12). To provide better adhesion, the backside of the shim was roughened with 220-grit sandpaper and rubbed with acetone to clean off any debris. The timber was also roughened with sandpaper to remove the previous adhesive and provide a better surface for the adhesive to grab onto. Loctite-426 adhesive was applied to the wood, and a 1-in. steel plate was used to apply pressure to the gage for 24 h. Initially, pressure had been applied to the gage by hand for approximately 2 min. Applying pressure for 24 h allowed the shim to stay in place as the adhesive cured to its full strength. In summary, the installation method was improved by roughening and cleaning the shim backing material and applying pressure until the adhesive reached its full strength.

The three top inoperable exterior gages were reattached using the improved installation method, and testing continued as usual for the remaining 800,000 cycles.

3.2.6 The Patch Method

Meanwhile, possible alternatives to attach strain gages to timber structures were discussed. A method, from now on termed the “patch method”, was chosen for evaluation. For clarity, the previous method will be termed the “shim method”. The basic idea of the patch method is to apply an adhesive patch, or coating, to the wood surface to fill in any voids or irregularities. After the patch cures, a foil strain gage is then applied to the patch using standard strain gage installation procedures. The procedure for the patch method is given in the following paragraphs.

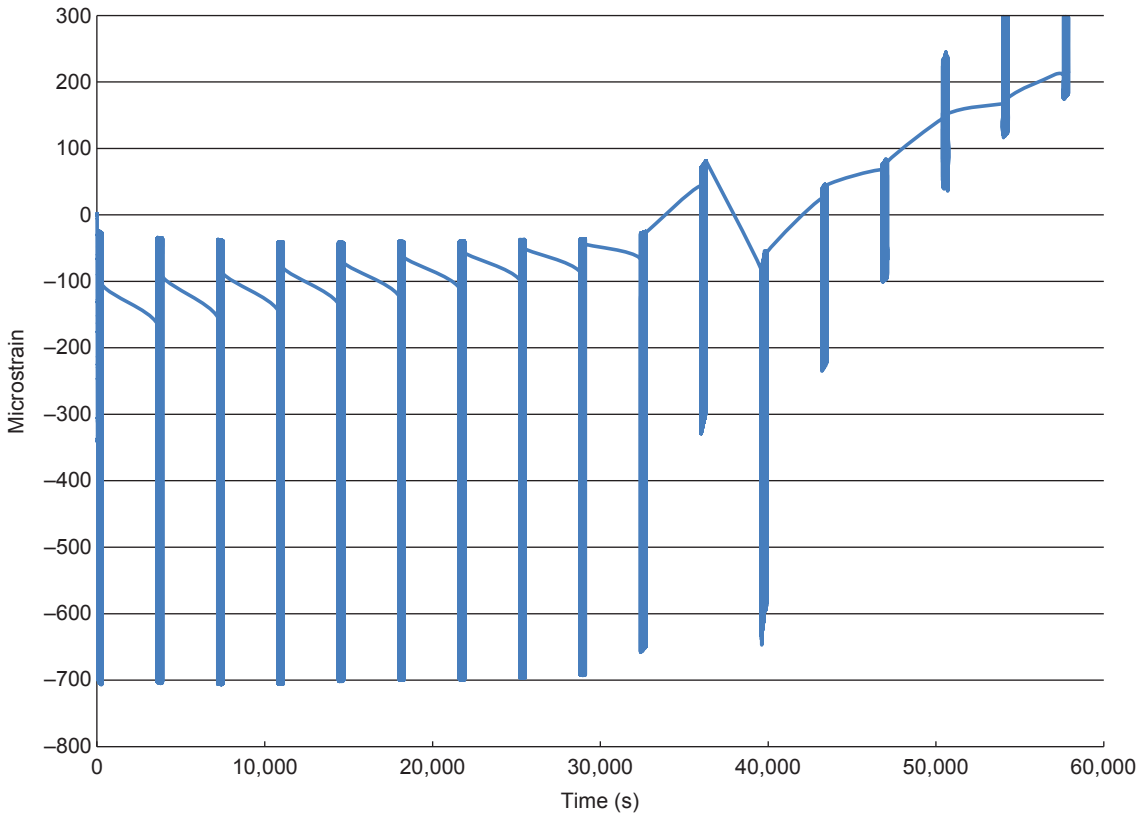

Figure 3.10. Top-A sensor response.

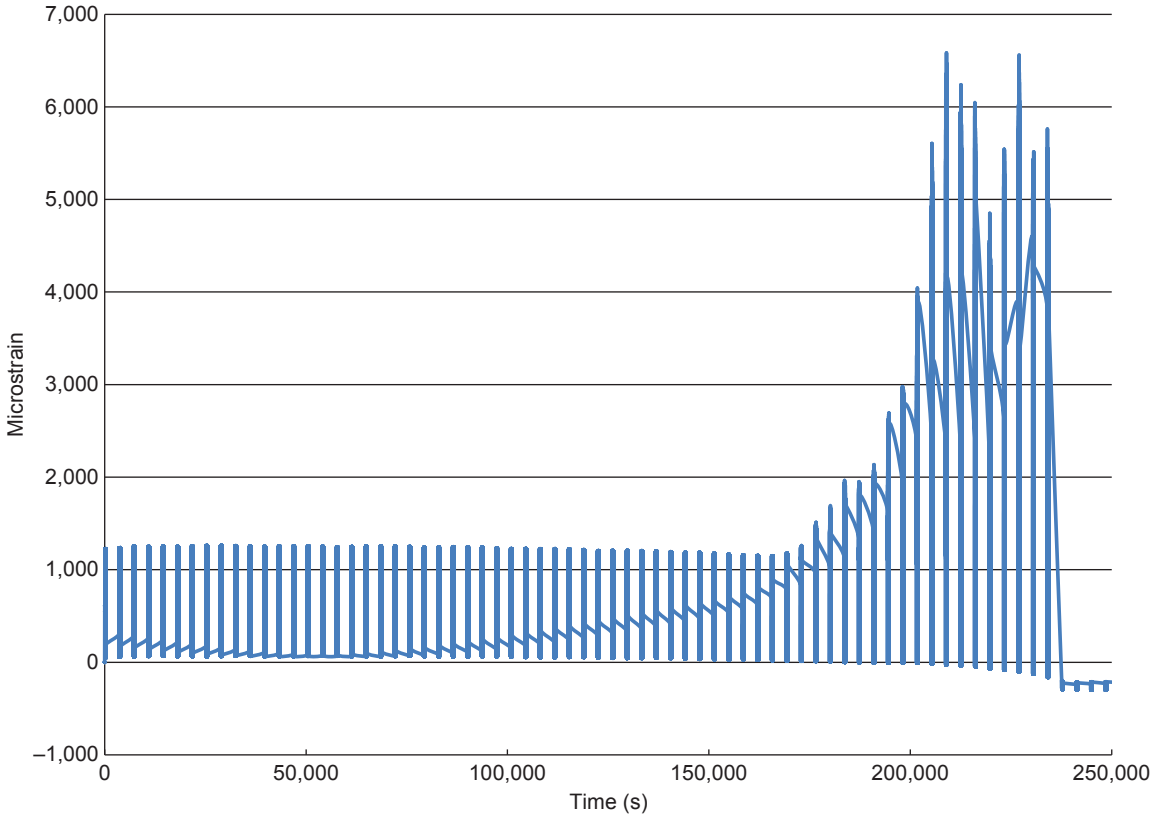

Figure 3.11. BL1-B sensor response.

Table 3.1—Sensor performance after 1 million cycles

Sensor[a]	Status[b]	Cycles at failure	Comments
Top-A	I	13,000	Offscale error, gage replaced at 200,000 cycles
TL1-A	O		
TL2-A	O		
BL1-A	O		
K-A	O		
Bottom-A	O		
Top-B	I	5,500	Unusual positive strains, gage replaced at 200,000 cycles
TL1-B	I	13,000	Unusual positive strains
TL2-B	I	50,000	Peak strain gradually dropping with time
BL1-B	I	110,000	Large strains
K-B	O		
Bottom-B	O		
Top-C	I	75,000	Small strains, gage reattached at 200,000 cycles
TL1-C	I	6,000	Erratic strain behavior throughout test
TL2-C	O		
BL1-C	I	800,000	Large strains
K-C	I	400,000	Offscale error
Bottom-C	O		
Top-west	O		Attached at 470,000 cycles using patch method
Middle	O		Attached at 470,000 cycles using patch method
Top-east	O		Attached at 470,000 cycles using patch method
Bottom-west	O		Attached at 470,000 cycles using patch method
Bottom-east	O		Attached at 470,000 cycles using patch method

[a]T, top; B, bottom; L1, laminate one; L2, laminate two; K, special tension lamination; A, B, C, Sections A, B, or C.
[b]I, inoperable; O, operable.

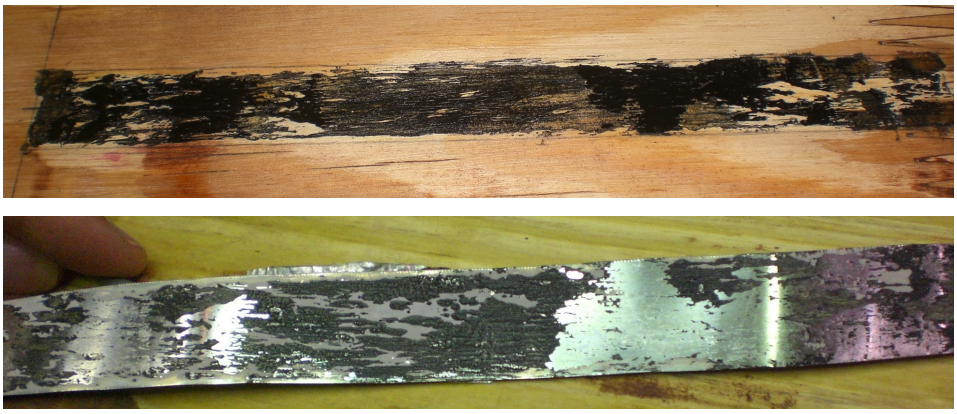

Figure 3.12. Adhesive on the wood surface (top) compared with shim (bottom).

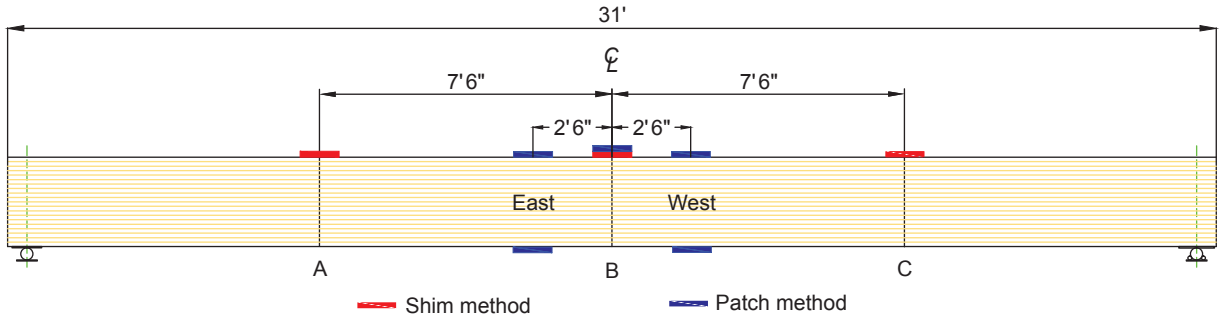

Figure 3.13. Shim and patch method locations.

The wood area where the gage was to be placed was sanded with 220-grit sandpaper to remove any oils or coatings on the wood surface and to develop a surface texture suitable for bonding.

Any debris on the wood surface was cleaned off with a brush or tape.

M-Bond AE-10 adhesive (Vishay Precision Group, Malvern, Pennsylvania, USA) was applied to the wood surface. The adhesive was worked into any voids and leveled to form a smooth surface. The adhesive was allowed to cure for 6 h at approximately 70 °F.

After the adhesive was cured, the patch was abraded with 320-grit sandpaper until the base material was exposed. Any debris was brushed off.

The layout lines for the gage were marked out using a ballpoint pen.

The foil gage was removed from its transparent envelope by grasping the edge of the gage backing with tweezers, and it was placed bonding side down on a chemically clean glass plate.

With PCT-2M gage installation tape, one end of the tape was tacked to the glass plate behind the gage and the tape was wiped forward onto the gage. The tape was carefully lifted at a shallow angle, bringing the gage up with the tape.

The tape–gage assembly was wiped onto the patch in the correct location.

One end of the tape was lifted at a shallow angle until the gage was free from the patch surface.

AE-10 adhesive was applied to the back of the gage and/or patch surface, and the gage was slowly brought back down over the layout lines.

A silicone gum pad and backup plate were placed over the gage installation. This allowed the force to be exerted evenly over the gage.

A dead weight or clamping pressure of 5 to 20 lb/in^2 was applied until the AE-10 adhesive cured (approximately 6 h).

After the adhesive cured, the pressure, gum pad, and backup plate were removed. The tape was removed by slowly pulling it back directly over itself.

If needed, butyl rubber and foil were applied to the top of the gage for protection.

At approximately 470,000 cycles, five additional gages were attached to Girder 1 using the patch method. The location of these gages and the replaced shim method gages are shown in Figure 3.13.

3.2.7 Status of the Exterior Shim and Patch Method Gages

Figures 3.14 and 3.15 illustrate the strain response caused by fatigue loading cycles for the shim and patch gages, respectively. The peak strain remained consistent and no unusual behavior was observed. In addition, the patch gages exhibited a consistent peak strain with little variation over time. As a result, based on Figures 3.14 and 3.15, both the exterior shim and patch gages performed well throughout the testing and further indicate that the improved preparation and installation technique for the shim gages ensured proper adhesion between the shim and wood surface. Furthermore, there was no visual or graphical indication of the patch gages not adhering to the wood surface and/or becoming damaged during the test.

The patch and shim gages provided similar strain readings in the constant moment region. Table 3.2 shows the comparison between gage types. Good agreement exists between the shim and patch gages particularly in the compression zone of the constant moment region. The gages in the tension zone, however, do not compare as well. Only the top shim gages were replaced at 200,000 cycles; the large percentage difference was probably caused by the Bottom-B shim gage not being replaced. To validate the results shown, a decision was made to test another girder in the lab with the improved shim and patch methods. By testing another girder, each gage type would be evaluated throughout the full 1 million cycles.

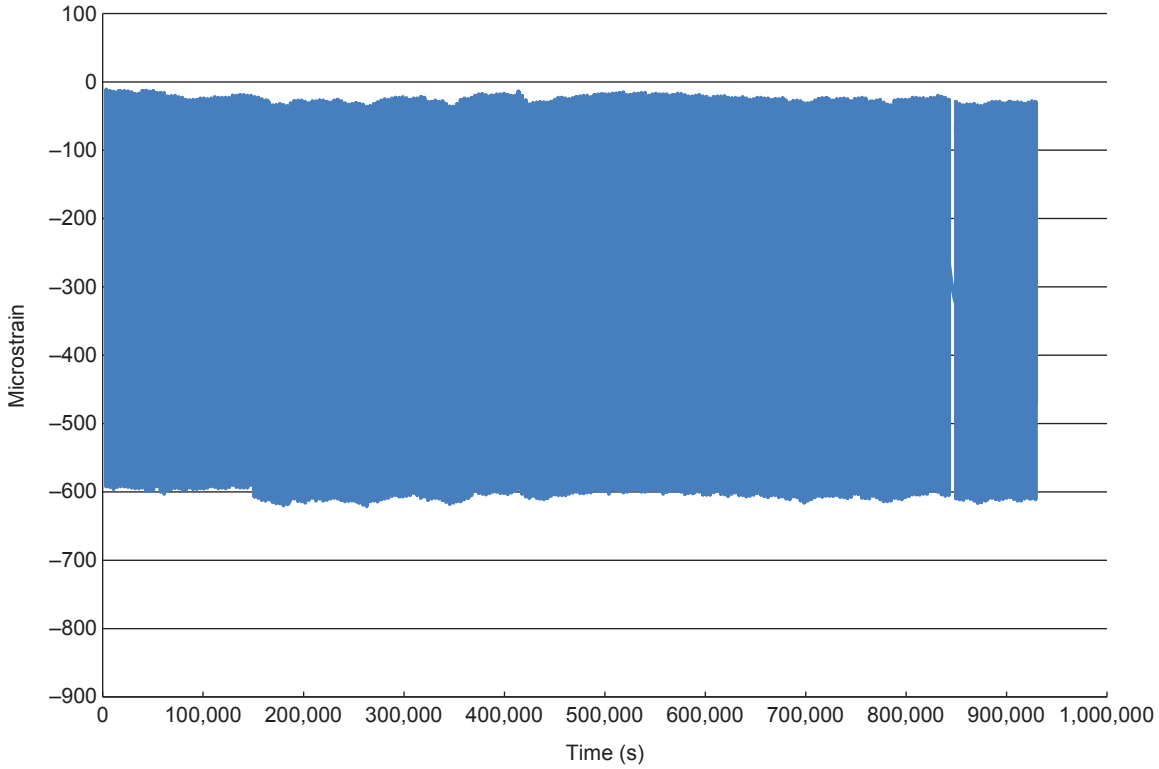

Figure 3.14. Top-C (shim) gage response.

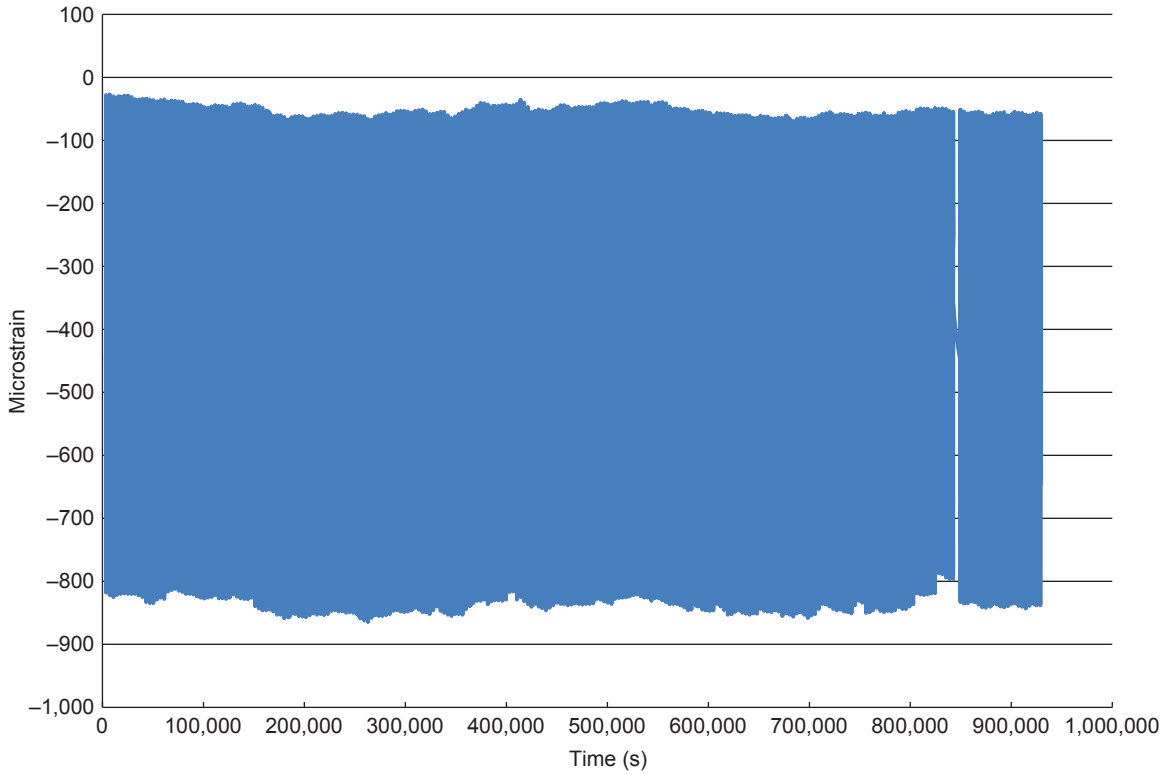

Figure 3.15. Top-east (patch) gage response.

Table 3.2—Constant moment region strain comparison

Patch gage	Average peak strain (microstrain)	Shim gage	Average peak strain (microstrain)	Percentage difference
Top-east	786	Top-B	775	1.4
Middle	784	Top-B	775	1.2
Top-west	810	Top-B	775	4.5
Bottom-east	856	Bottom-B	1,020	16.1
Bottom-west	911	Bottom-B	1,020	10.7

3.3 Girder 2

Girder 2 was fabricated to the same cross section, length, and beam layup as Girder 1. The differences between Girder 1 and Girder 2 were the species, treatment, and sensor layout. Girder 2 consisted of Douglas-fir laminates and was pressure treated with pentachlorophenol after the girder was constructed. The purpose of pressure treating the girder was to observe how exterior gages adhered to treated timber. If the gages performed well, they would have the potential to be used on timber bridges already in service. The sensor locations of Girder 2 are shown in Figure 3.16. The sensor locations remained the same as Girder 1; however, half of the sensors were installed using the patch method and the other half were installed using the shim method. In addition to the strain gages, moisture sensors were installed at the three cross sections A, B, and C (Fig. 3.16b).

3.3.1 Testing Program

For consistency, Girder 2 was tested using the same testing program as Girder 1 (see section 3.3). After fatigue testing, Girder 2 was then subjected to a load of 44 kips to evaluate sensor performance at loads exceeding service levels.

3.3.2 Results

3.3.2.1 Gage Survivability

Table 3.3 lists the status of the gages after 1 million cycles. The gages installed using the shim method and the exterior patch method gages were operable throughout the test and did not experience the unusual behavior observed in Girder 1. The interior patch method gages, however, were inoperable throughout most of the test.

After testing was completed, the girder was cut open and the interior gages examined. All the interior patch method gages failed in the same manner as shown in Figure 3.17. The fragile connection between the wire and the gage failed for a couple reasons. One reason was the lack of stress relief on the wire–gage connection. The gage and wire–gage connections were coated with polyurethane for protection. The polyurethane coating adhered the connection to the wood, inducing stress on the connection under loading. Furthermore, the interior gages did not come prewired; therefore, the wires had to be soldered to the leads on the gage to establish the connection. The exterior gages came prewired and the wire–gage connection was less fragile compared with the soldered connection on the interior gages. In short, the lack of stress relief on the gage and a fragile soldered connection led to the gage failure.

3.3.2.2 Strain Response and Comparison

Figures 3.18 and 3.19 illustrate the typical strain response caused by fatigue loading cycles for the shim and patch gages for Girder 2, respectively. As shown in these figures, some of the gages do not recover to zero strain. This behavior is known as “drift” and is common in foil strain gages. When drift is present, the strain range should be evaluated instead of peak strain. The strain range, shown in Figures 3.20 and 3.21, is calculated by subtracting the minimum strain from the maximum strain. The consistency of the strain range plots indicates the gages survived the fatigue loading.

The peak strain ranges from the exterior shim and patch gages were compared to observe any differences (Table 3.4). The percentage differences between gage types ranged from 1.5% to 18.4%. In addition, the patch method gages recorded slightly higher strains compared with the shim method gages with the exception of sensor location Top-C. Overall, the two gage types compared reasonably well.

3.3.2.3 Theoretical Strain Comparison

According to the published graded 24F-V8 DF/DF girder characteristics for loads applied perpendicular to the wide faces of the laminations, the modulus of elasticity (MOE) was estimated to be 1,800 kips/in^2 (APA 2008). Thus, theoretical peak strains were calculated using basic beam theory formulas, assuming that the girder was loaded in the elastic range and both compressive and tensile flexural properties are the same. In Table 3.5, the estimated strains at each operable gage location are compared with the experimental strains. The percentage differences ranged from minimal to 27.4%. Furthermore, the experimental peak strains were consistently lower than the theoretical values.

3.3.2.4 Experimental Neutral Axis

At the three cross sections, the position of the neutral axis based on the exterior gages was plotted with time. The neutral axis position stayed fairly consistent throughout

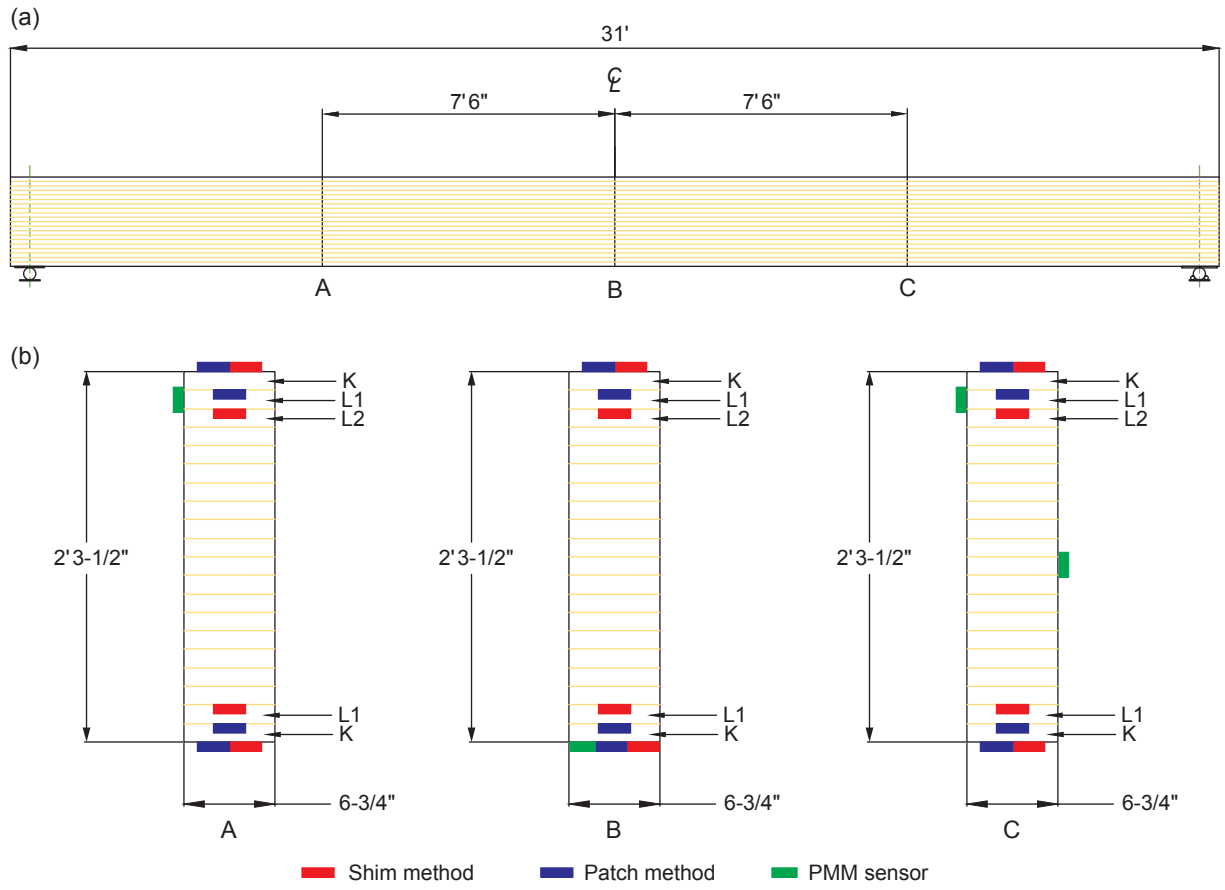

Figure 3.16. Gage locations on Girder 2: (a) location along the length; (b) gage location at cross sections A, B, and C.

the fatigue testing (Fig. 3.22). The neutral axis position is not coincident with the geometrical center of gravity (that is, 13.75 in.). At midspan, the neutral axis location was approximately 0.5 in. above the center of gravity. The difference was attributed to the orthotropic nature of wood.

3.3.2.5 Ultimate Load Test

To study the behavior of the sensors under high strains, Girder 2 was loaded to almost double the load used during fatigue testing (44 kips). This testing allowed for evaluation of the static performance under overload conditions.

The operable gages at the end of the fatigue test were still functioning at the end of the ultimate load test. The stress–strain plot of the exterior shim and patch gages is shown in Figure 3.23. As shown, the gages demonstrated linear elastic behavior throughout loading. In addition, the MOE was determined by plotting a linear regression trend line. The MOE ranged from 1,466 to 1,802 kips/in^2; furthermore, the compressive MOE was higher than the tensile values.

3.3.2.6 Moisture Results

Figure 3.24 shows the MC with time plot for data obtained from the PMM sensors. In addition, the plot shows the MC readings obtained from a conventional moisture meter (RDM3, Delmhorst Instrument Co., Towaco, New Jersey, USA) using 3-in. Teflon (Chemours Co., Wilmington, Delaware, USA)-insulated pins hammered to a depth of approximately 1 in. at the beginning and end of the fatigue testing. According to the PMM sensors, the initial MC of Girder 2 ranged from 9.4% to 10.7%. The MC gradually decreased to a range of 7.2% to 8.5% by the end of the test. The EMC corresponding to the room conditions (69 °F and 40% relative humidity) was 7.7%.; therefore, a decrease in MC was expected because the girder was drying out to establish equilibrium with the environment. Furthermore, the PMM sensors consistently recorded MCs below the readings obtained from the Delmhorst moisture meter. However, the moisture meter did follow the same trend as the PMM sensors.

Table 3.3—Sensor performance at 1 million cycles

Sensor[a]	Status[b]	Cycles at failure	Comments
Shim method			
TL1-A	O		
K-A	O		
Bottom-A	O		
Top-B	O		
TL1-B	O		
BL1-B	O		
Bottom-B	O		
Top-C	O		
TL2-C	O		
BL1-C	O		
Bottom-C	O		
Patch method			
Top-A	O		
TL2-A	I	250	No connection
BL1-A	I	0	Inoperable upon arrival
Bottom-A	I	0	Damaged during installation
Top-B	O		
TL2-B	I	2,000	No connection
K-B	I	0	Inoperable upon arrival
Bottom-B	O		
Top-C	O		
TL1-C	I	32,000	No connection
K-C	I	1	No connection
Bottom-C	O		

[a]T, top; B, bottom; L1, laminate one; L2, laminate two; K, special tension lamination; A, B, C, Sections A, B, or C.
[b]O, operable; I, inoperable.

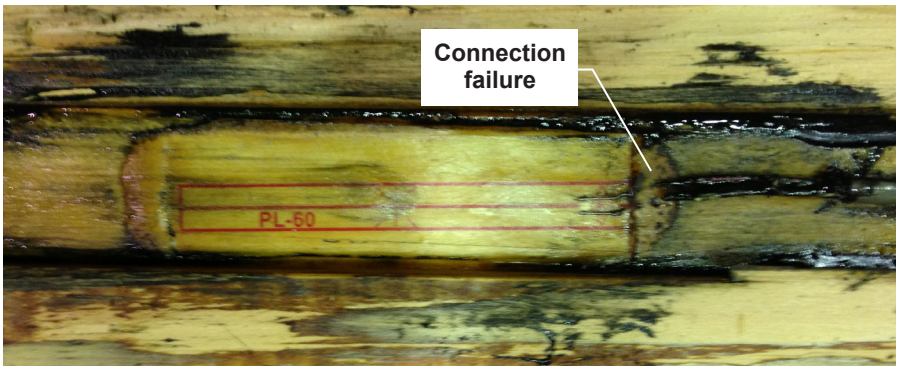

Figure 3.17. Wire–gage connection failure.

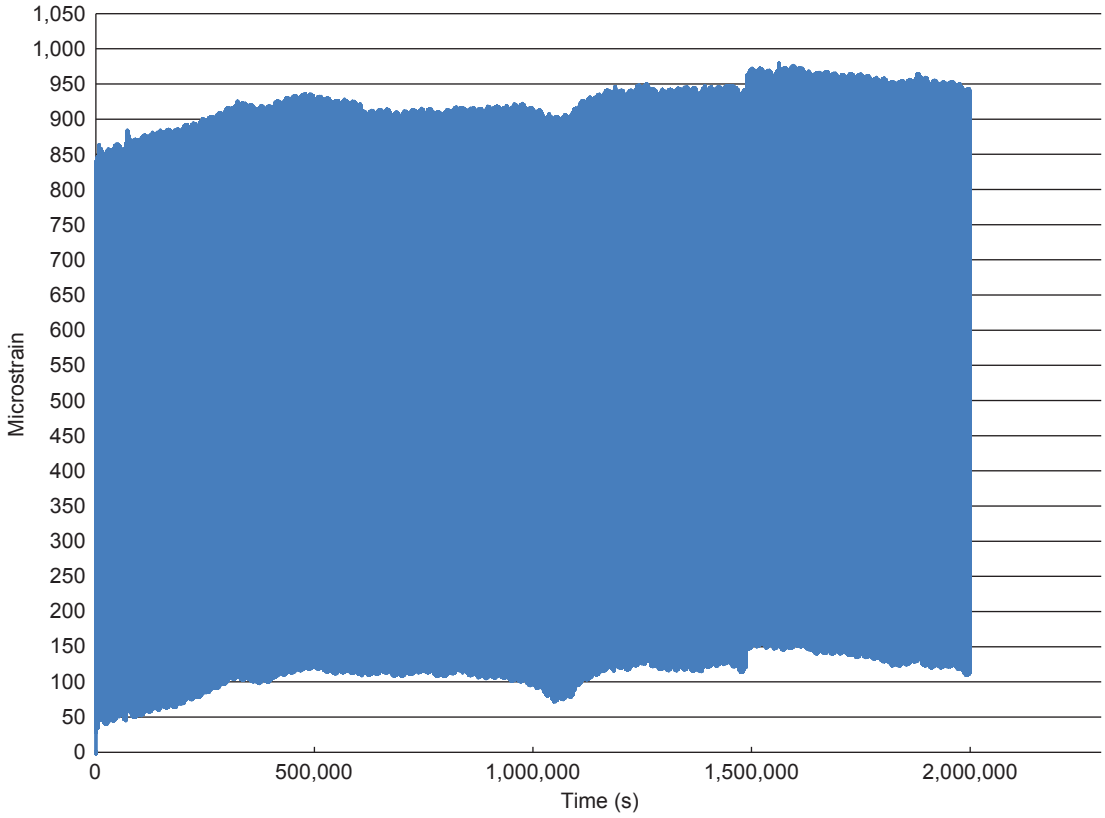

Figure 3.18. Bottom-A shim gage response.

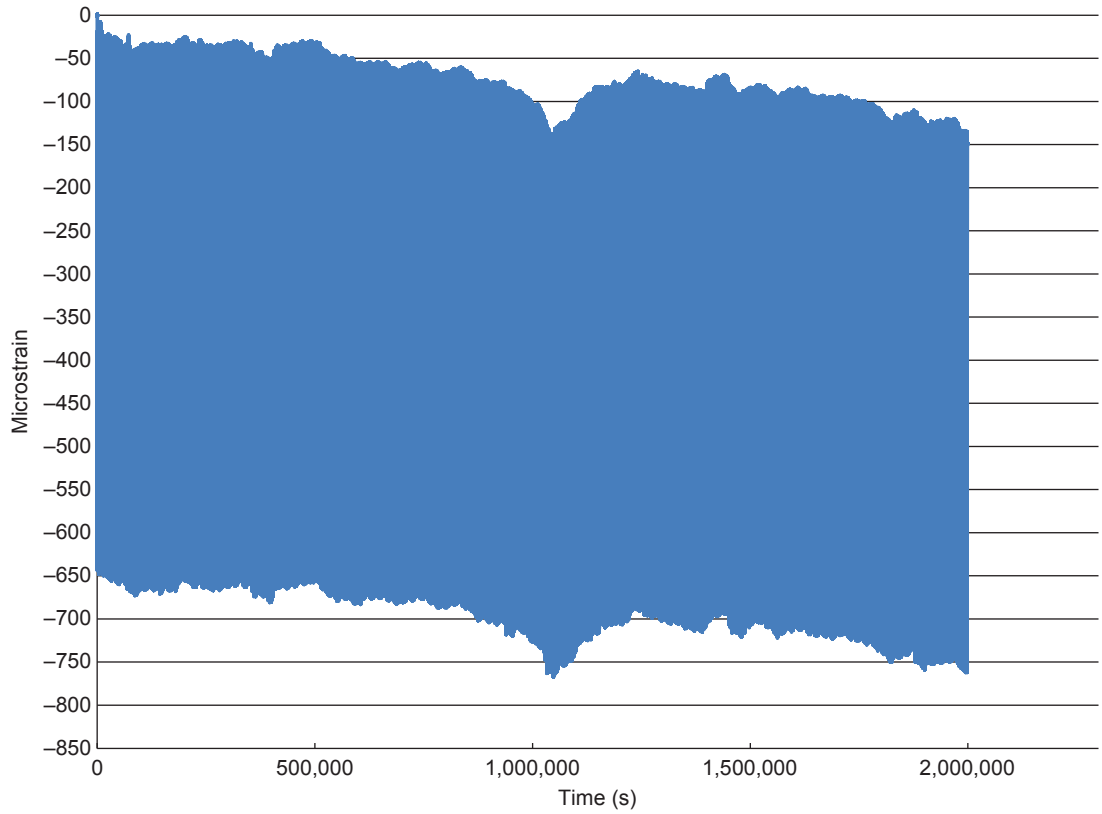

Figure 3.19. Top-C patch gage response.

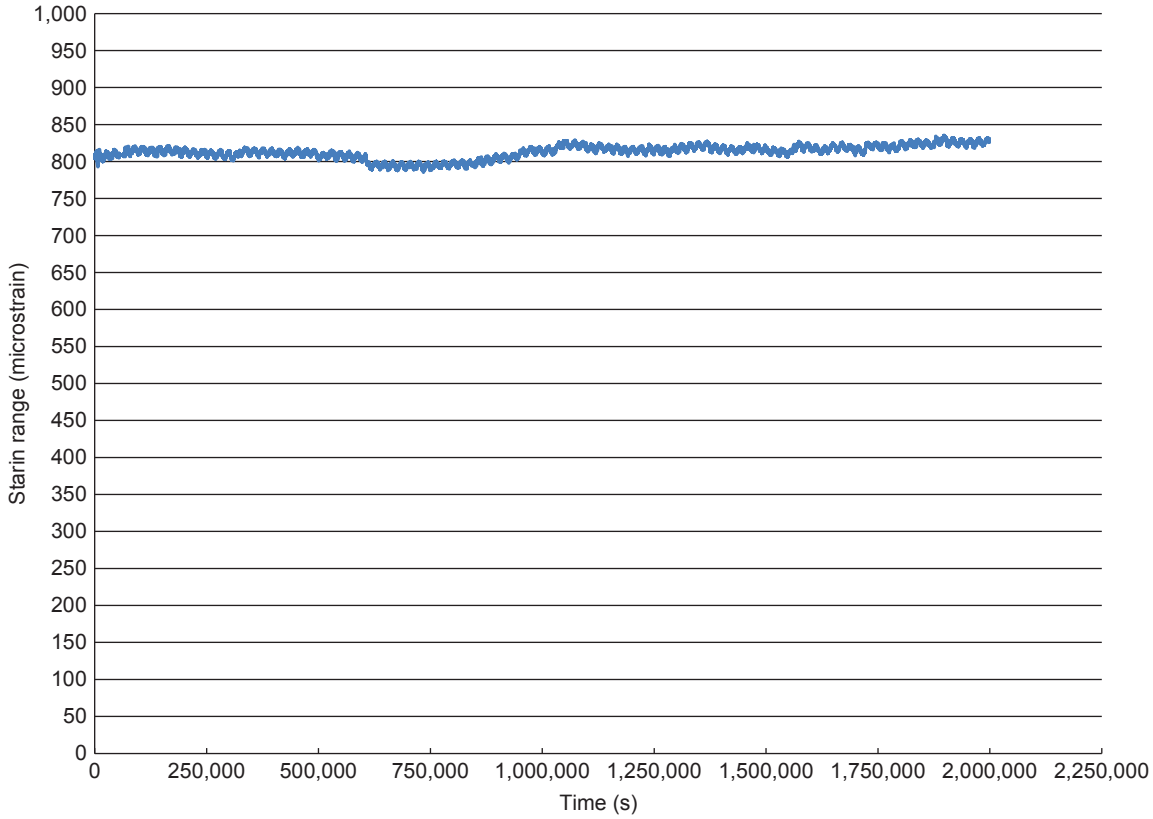

Figure 3.20. Bottom-A shim strain range.

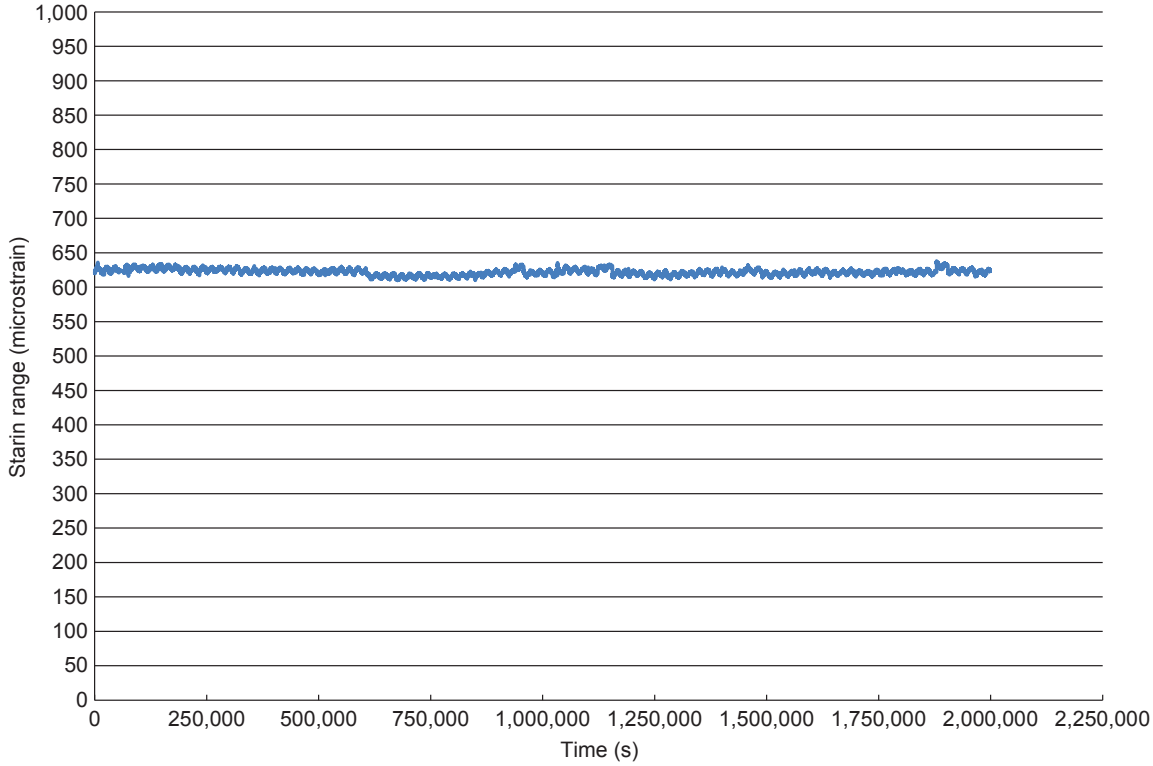

Figure 3.21. Top-C patch strain range.

Table 3.4—Exterior patch method and shim method strain comparison

Sensor location	Shim gage average strain range (microstrain)	Patch gage average strain range (microstrain)	Percentage difference
Top-A	512	606	18.4
Bottom-A	819	NA[a]	–
Top-B	811	865	6.6
Bottom-B	867	948	9.4
Top-C	638	628	1.5
Bottom-C	645	710	10.0

[a]NA, gage damaged during installation.

Table 3.5—Theoretical compared with experimental peak strain

Sensor[a]	Theoretical peak strain (microstrain)	Experimental peak strain (microstrain)	Percentage difference
Shim method			
Top-A	705	512	27.4
TL1-A	622	564	9.3
K-A	686	685	0.1
Bottom-A	705	819	16.1
Top-B	987	811	17.9
TL1-B	871	803	7.8
BL1-B	808	769	4.8
Bottom-B	987	867	12.2
Top-C	705	638	9.5
TL2-C	584	437	25.1
BL1-C	611	604	1.1
Bottom-C	705	645	8.5
Patch method			
Top-A	705	606	14.1
Top-B	987	865	12.4
Bottom-B	987	948	4.0
Top-C	705	628	11.0
Bottom-C	705	710	0.7

[a]T, top; B, bottom; L1, laminate one; L2, laminate 2; K, special tension lamination; A, B, C, Sections A, B, or C.

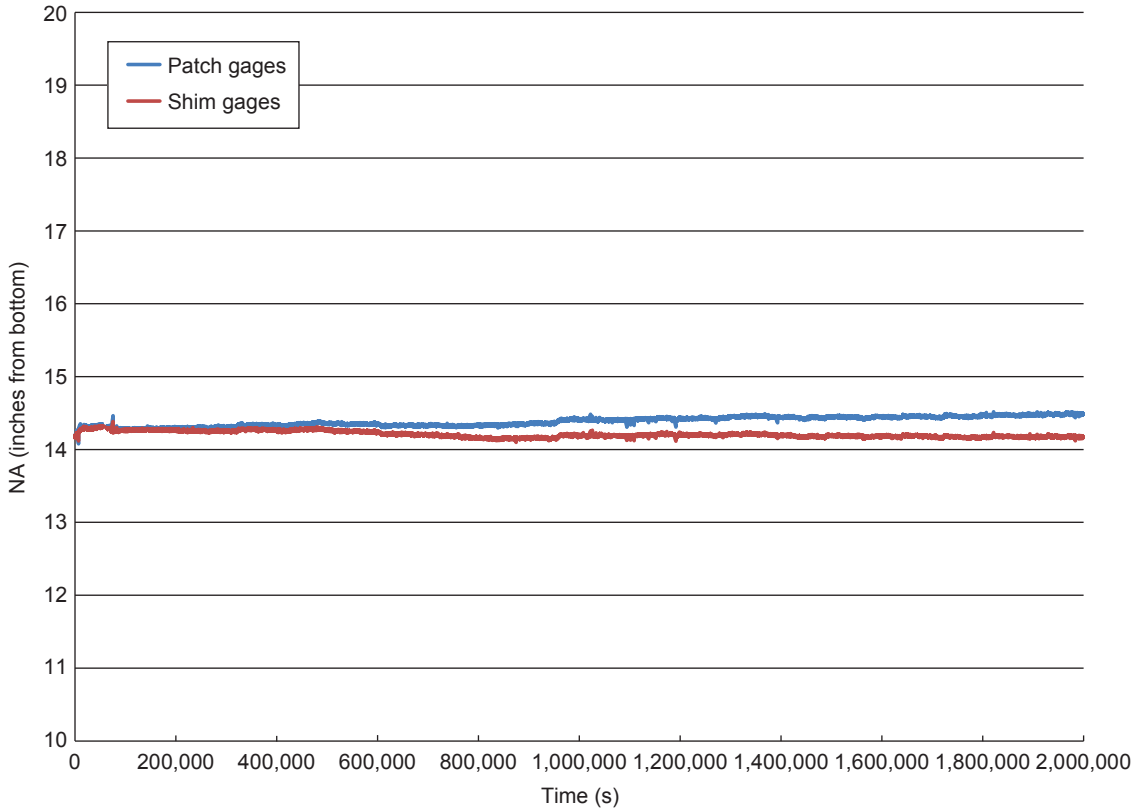

Figure 3.22. Neutral axis (NA) location.

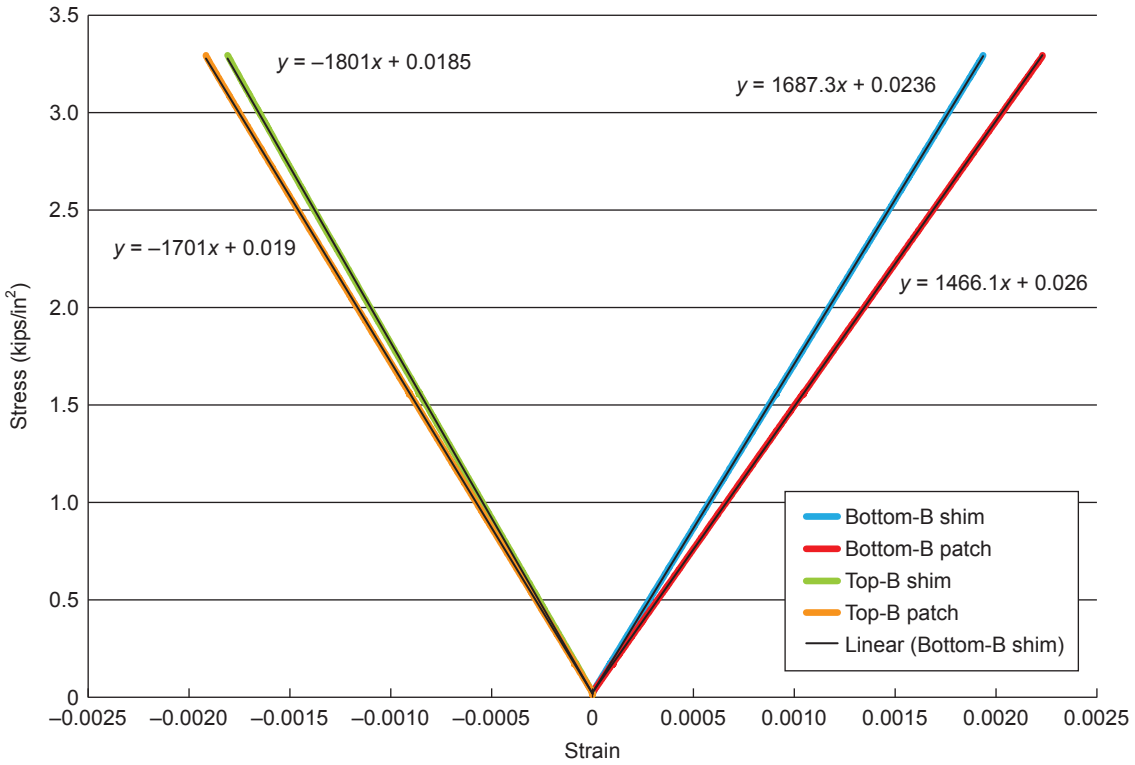

Figure 3.23. Section B stress–strain plot.

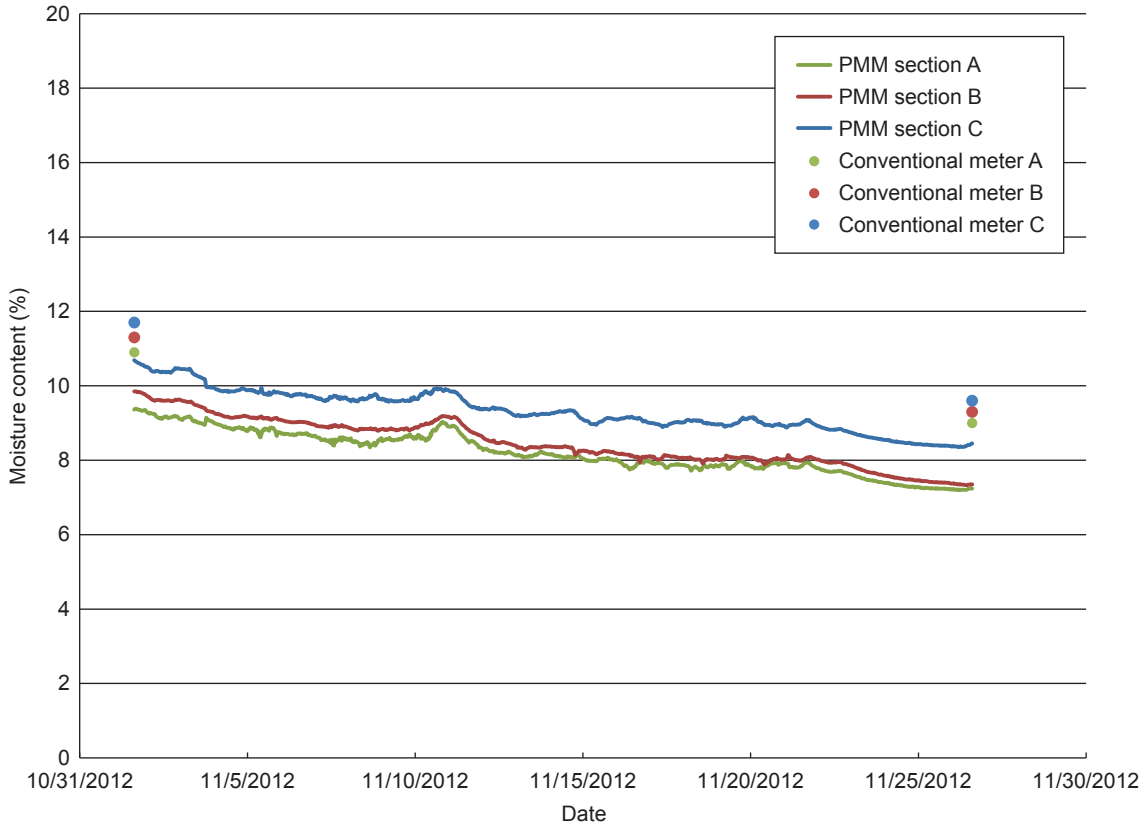

Figure 3.24. Changes in moisture content during fatigue test (PMM, point moisture measurement).

4 Summary, Conclusions, and Recommendations

4.1 Summary

The focus of this study was to continue advancing timber-specific sensing capabilities. Three commercially available moisture sensors were investigated through testing on small-scale specimens. The three evaluated sensors were a relative humidity–temperature sensor, a PMM sensor, and an EMS. The specimens were subject to varying environmental conditions to evaluate the survivability and accuracy of measurements. The results of the test show the relative humidity–temperature sensor provided the most accurate readings compared with a commercially available moisture meter. Furthermore, the sensor was able to read MCs near 20%, a common threshold for incipient decay in timber structures. However, the sensor was unable to be wired into a data logging system capable of reading other sensor types, a necessary feature in structural health monitoring. As a result, the PMM sensor was chosen for further evaluation. The PMM sensor offered reasonable results but was unable to read near 20% MC. Future calibration of the system is required to obtain more accurate measurements. The system calibration would entail altering the equations relating MC, electrical resistance, wood species, and temperature to match MC measurements obtained from gravimetric results and/or a moisture meter.

Two full-scale glulam timber girders, equipped with strain and moisture sensors, were constructed and tested to further evaluate the operability of the sensors. The girders were assembled at a local glulam manufacturing facility. Strain gages were installed on four internal laminates at three cross sections. A technique to embed the gages was developed and integrated into the fabrication process. Regarding survivability, the method of instrumenting the laminates and assembling the girder was successful because all 12 interior gages were operable for Girder 1.

Girder 1 was tested under repeated loading to evaluate the performance of the sensors. The girder was tested to one million cycles with a peak load of 24 kips. The load was distributed to two point loads, simulating a typical truck loading. Shortly into testing, several gages demonstrated nontypical behavior. A conclusion was made that the preparation of the gages was inadequate, resulting in insufficient adhesion between the gage and the wood surface. An improved technique, termed the shim method, was developed and proved to be successful through the remainder of the test.

An alternative to the shim method, termed the patch method, was developed and implemented into Girder 2. Girder 2 was fabricated using both the shim and patch methods. Upon construction, the patch method gages were inoperable because of a fragile wire–gage connection. The fragile connection could be avoided in the future by using prewired gages and providing stress relief on the connection. Girder 2 was tested using the same testing program as Girder 1 (that is, 1 million cycles, 24-kip peak load). The test data indicated that both gage types provided similar results. The percentage differences between the gages ranged from 1.5% to 18.4%. The larger percentage difference can be attributed to surface irregularities on the wood surface (for example, grain orientation). The gages compared reasonably well with theoretical strains calculated by beam theory formulas. The gages were consistently higher than the theoretical strains, differing by as much as 27%. The difference can be credited to the uncertainties in the estimated MOE caused by the orthotropic nature of wood materials. In addition to the fatigue test, an ultimate test was performed to subject the gages to strains above service levels. Both gage types survived the ultimate test and demonstrated linear elastic behavior throughout loading. In summary, with the exception of the failed connection of the interior patch gages, both gages survived the fatigue loading and provided reasonable and consistent results throughout testing.

In addition to the strain gages, the PMM sensors were installed on Girder 2 and monitored throughout the fatigue test. The MC decreased about 2% throughout the test. A moisture meter was used to compare the results. The moisture meter demonstrated the same trend (2% decrease); however, the values were consistently higher than the PMM values by approximately 1%. One explanation for the difference in MC measurements is the insertion depth of the pins. The moisture meter is equipped with insulated pins that measure the electrical resistance only at the tip. Conversely, the PMM uses noninsulated screws, measuring the resistance through the whole length of the screw. Isolating the tips of the screws by either coating the screw or using a small tube would probably provide more accurate measurements.

4.2 Conclusions

The following are the general conclusions of the study.

As a result from the small-scale moisture testing, the PMM sensor was chosen as the superior option for the following reasons:

The sensor was successfully wired into a data logging system capable of reading other sensor types.

The installation procedure was easier compared with the other sensor types. The sensor did not require predrilling or sealing, thus saving time and difficulties in field installation.

Relating electrical resistance to MC has been around for years and is tried and trusted in the timber industry. Most moisture meters used in timber bridge inspections rely on this technology.

The sensor responded well to varying environmental conditions, indicating obvious trends in moisture gain or loss.

Reasonable accuracy was achieved particularly at lower MCs. A drawback of the sensor is its inability to accurately measure MCs near 20%.

The rigidity of the sensor made it unlikely to become damaged under repeated loading.

One caveat to this sensor type would be the use of salt preservatives in the wood. An uncoated tip would have corrosion issues; however, use of coated pins would greatly decrease the potential for corrosion and/or other problems.

Two methods for attaching and embedding foil strain gages to timber were developed (shim and patch). Both methods were successfully integrated into the glulam manufacturing process.

During the fatigue test, both gage types validated each other by measuring similar strains. In addition, the strains were higher than predicted values; however, this can be attributed to difficulties in estimating MOE.

The strain ranges of the shim and patch method gages were consistent throughout the fatigue test. Therefore, a conclusion was made that repeated loading did not cause damage to the gages.

4.3 Recommendations

Based on this study, a recommendation is made to use the PMM sensor to measure the MC in smart timber bridge applications. Furthermore, it is recommended to calibrate the system to acquire more accurate readings, particularly near 20% MC. The calibration would require altering the equations relating the MC, electrical resistance, wood species, and temperature to match MC measurements obtained from gravimetric results and/or a moisture meter. In addition, altering the wiring schematic discussed in Chapter 2 may aid in the calibration. Experimenting with different excitation voltages and reference resistors may provide greater accuracy around 20% MC.

Although the shim and patch method gages provided similar results, a recommendation is made to use the shim method in future timber bridge applications. The shim gages required significantly less time to install compared with the patch gages. The time required for the patch coating to cure would add approximately 6 h to the glulam fabrication process and/or field installation.

5 Acknowledgments

The research team acknowledges all those who assisted with the successful completion of this work. A special thank you to John Foreman and Alamco of Albert Lea, Minnesota, for their assistance and cooperation with beam fabrication and sensor integration and Doug Wood at Iowa State University for his assistance with the laboratory testing of all specimens and sensors.

6 References

APA. 2008. Glulam design specification. Tacoma, WA: APA – The Engineered Wood Association.

ASTM. 2007. D4442-07. Standard test methods for direct moisture content measurement of wood and wood-base materials. West Conshohocken, PA: American Society for Testing and Materials International.

ASTM. 2008. D4444-08. Standard test methods for laboratory standardization and calibration of hand-held moisture meters. West Conshohocken, PA: American Society for Testing and Materials International.

Dai, G.; Ahmet, K. 2001. Long-term monitoring of timber moisture content below the fiber saturation point using wood resistance sensors. Forest Products Journal. 51(5): 52-56.

Dyken, T.; Kepp, H. 2010. Monitoring the moisture content of timber bridges. In: Malo, K.A.; Kleppe, O.; Dyken, T., eds. Proceedings, international conference timber bridges (ICTB). Lillehammer, Norway. September 12-15, 2010. Trondheim, Norway: Tapir Academic Press: 223-236.

Forest Products Laboratory. 1999. Wood handbook—Wood as an engineering material. General Technical Report FPL-GTR-113. Madison,WI: U.S. Department of Agriculture, Forest Service, Forest Products Laboratory. 463 p.

Forest Products Laboratory. 2010. Wood handbook—Wood as an engineering material. General Technical Report FPL-GTR-190. Madison,WI: U.S. Department of Agriculture, Forest Service, Forest Products Laboratory. 508 p.

Pfaff, F.; Garrahan, P. 1984. Moisture content correction tables for resistance-type moisture meter (revised temperature corrections). Report SP511E. Ottawa, Ontario, Canada: Forintek Canada Corp.

Phares, B.M.; Wipf, T.J.; Deza, U. 2010. Evaluation of techniques for embedding and attaching FBG sensors to new glulam bridge members. Ames, IA: Iowa State University, Bridge Engineering Center.

Wacker, J.P.; Joyal, M.R.; Murphy, J.F.; Wang, X. 2007. Monitoring the performance of timber bridges over the long term. Proceedings, 2007 Mid-Continent Transportation Research Symposium. Ames, IA. August 2007. Ames, IA: Iowa State University.

Yeo, T.L.; Eckstein, D.; McKinley, B.; Boswell, L.F.; Sun, T.; Grattan, K.T.V. 2005. Demonstration of a fibre-optic sensing technique for the measurement of moisture absorption in concrete. Institute of Physics Publishing. 15(2): N40-N45.